

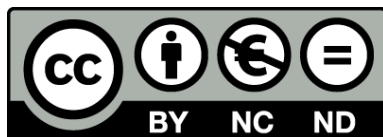


UNIVERSITAT DE
BARCELONA

Field-effects on single molecular circuitry

Electronic transport from synthetic to biological models

Albert Cortijos i Aragonès



Aquesta tesi doctoral està subjecta a la llicència [Reconeixement- NoComercial – SenseObraDerivada 3.0. Espanya de Creative Commons.](#)

Esta tesis doctoral está sujeta a la licencia [Reconocimiento - NoComercial – SinObraDerivada 3.0. España de Creative Commons.](#)

This doctoral thesis is licensed under the [Creative Commons Attribution-NonCommercial-NoDerivs 3.0. Spain License.](#)

Preface

Objectives

Inspired by the proposal that single molecules will be functional elements of future nanoelectronics and Spintronic devices, there exists considerable interest in understanding charge transport in individual molecular backbones. To investigate charge transport in single-molecule devices, in the presented thesis is exploit scanning tunneling microscopy-based approaches in the Scanning Tunneling Microscope *Break-Junction* technique designed by Xu and Tao in 2003, incorporating the novel implementation of two force fields stimuli: external magnetic and electric fields.

The magnetic effects over the electron transport at single-molecular level offer a new added value to the Molecular Electronic field and its future applications and miniaturization of electronic devices and open the gates to the field of quantum computing. The main propose of this thesis is the contribution to the development of practical and applicable devices, for this reason working at Room Temperature is one of the cornerstones for the presented project, representing a breakthrough respect the previous works which mixed magnetic fields and Molecular Electronics. Under this premise, is presented a study of three different kinds of molecules, two paramagnetic classes of molecules which are *metal complexes* and *metalloporphyrins*, being the latter a significant approach to mimicking natural structures; and the third kind of molecule, a *chiral diamagnetic peptides*, exploiting natural structures with relevant electronic properties.

On the other hand, the electric fields, will be used to study and control basic mechanisms in chemical catalysis at the single-molecular level, employing the *Diels-Alder reaction* as testing reaction due its simplicity and the extended theoretical studies behind.

Structure

The presented thesis contains seven **Chapters**. After the **Introduction** which conforms the *Chapter 1*, is divided in three big parts. The two first parts are associated to both employed force fields, the magnetic field (from *Chapter 2* to *Chapter 4*) and the electric field (*Chapter 5*) and finally the third part contains the **Conclusions of the Thesis** (*Chapter 6*) and associated **Future Perspectives** (*Chapter 7*). Below is listed a brief description of each Chapter:

- ***Chapter 1***: Is an introduction about the following concepts: Molecular Electronics, its history and state-of-the art of the different techniques and examples; the Electron transport phenomena in nanoscale junctions; the Scanning Tunneling Microscopy Technique and finally the Spintronics main concepts as well as its state-of-the-art related to the relevant application for this thesis. The second aim of the introduction, apart from explaining the required background concepts, is to be used as a reference compendium of the most important and novel references of each explained topic, for this reason the amount of literature citations is extensive.
- ***Chapter 2***: Is presented the study performed at room-temperature based on spin-dependent transport in single-molecule devices employing on thermal spin-crossover metal complexes.
- ***Chapter 3***: As a first part is presented a novel way to form highly conductive and tunable molecular wires exploiting supramolecular chemistry schemes. This novel platform of wiring individual metalloporphyrins mimics the way nature exploits these systems by orienting the perpendicular porphyrin axis as the easy axis for electron/energy transfer. Then are presented the spin-dependent transport experiments using paramagnetic metalloporphyrins and employing the new developed technique at room temperature.
- ***Chapter 4***: Is focused on spin-selectivity induced by electron transport through chiral molecules, replacing the paramagnetic character of the device's central molecules previously studied. A new method to quantify the spin-polarization power of chiral molecules is presented using a junction of amino-acid peptide chiral structures, coupled to an Au surface and to a magnetized Ni contact.
- ***Chapter 5***: Here is studied the catalysis of the Diels-Alder under the application of external electronic fields, in different orientations and strength. The study will be performed by delivering an oriented electric field-stimulus across two reactants: a diene, attached to the STM tip electrode and a dienophile attached to the substrate electrode.
- ***Chapter 6***: Corresponds to the general conclusions of the thesis extracted from the most relevant conclusions of each Chapter and relating them.

- **Chapter 7:** Here are summarized all the emerged ideas during the thesis, which can be used as a continuation of the performed research.

From *Chapter 2* to *Chapter 5*, each Chapter contains one or two topics, and for each one there is: a specific **introduction**; a detailed description of the employed **set-up**, since the versatility of the employed STM-BJ approach and the specific experimental requirements due the force fields application, and also there are the **objectives** with the **experimental conditions** along with the **summary** included as *publication*. Finally there are the detailed **Conclusions** exclusively for the Chapter.

This thesis also contains **Appendices**, which gathers: a **Summary** of the thesis (*in Catalan*), a compendium of useful **Symbols and Acronyms**, **Additional technical details** (including *additional information of the used STM-BJ approaches*, *data capture and processing* as well as *details of the single molecule experiments preparation*, and also a brief description of the employed Low Temperature STM) and as a final section the list of the **Publications** achieved during the PhD.

Preliminary concepts

- ▶ **Nanoscience/Nanotechnology** | Applied human's knowledge based on the manipulation of the matter and the study of any phenomenon occurred ranging from the atomic to the supramolecular scale, thus it is limited from 1 to 100 nm.
- ▶ **Spintronics** | Ability of injecting, manipulating and detecting electron spins into solid state systems.
- ▶ **Nanometer(nm)** | 10^{-9} meters.
- ▶ **Molecular Electronics** | Science and technology involved on the understanding, design, and developing of electronics devices based on molecules.
- ▶ **Molecular junction** | Electrode–molecule–electrode structure built from an attached molecule between two electrodes.
- ▶ **Contact geometry** | The atomic-scale geometry of an electrode, and the binding site and orientation of a molecule on the electrode.
- ▶ **Molecule-electrode contact** | Contact between a molecule and an electrode which provides sufficient and stable electronic coupling between the molecule and the electrode.
- ▶ **Quantum Point Contact (QPC)** | Small constriction between two conducting regions through which electrons traverse ballistically and suffer a quantum waveguide effect.
- ▶ **Conductance quantum unit** | Basic unit of conductance given by $G_0 = 2e^2/h$, where G is conductance, where e is the electron charge and h is Planck Constant.
- ▶ **Redox molecule** | Molecule that can be reversibly oxidized or reduced via electron transfer between the molecule and electrodes

Chapter 1

Introduction

1.1 The discipline: *Molecular electronics*

Molecular Electronics... This concept has a very intuitive meaning, since in fact, can be defined by itself as the merely mixing of two concepts: Electronics and Molecules. Electronics is understood as the branch of human's knowledge based on controlling electrical energy electrically, in which the electrons have a fundamental role. Therefore, by analogy, Molecular Electronics is the field in which molecules are used to control and manipulate the electrical current behavior similar to what is offered by the micro or macro electronic devices.¹ Such concept implies that molecules can mimic the behavior of some of today's microelectronic components as active (switching, sensing, transistors, etc.) or passive (resistors, current rectifiers, surface passivants, etc.) elements in electronic devices,² therefore the aim is to replace such microelectronics components by single-molecules and incorporate them as functional parts in macroscale electronic devices to increase the efficiency due the reduced size since they are molecules.^{3,4}

In fact, building electronic devices using individual molecules is one of the ultimate goals in Nanotechnology. Furthermore, in parallel exist other non-applied research fields focused on the understanding of the electron transport through molecules as a conductor, trying to understand the molecules' role in the molecular circuits. And, maybe, this double contribution is the most remarkable issue given by Molecular Electronics, because not only moved the researchers to develop several novel techniques but also represents a unique opportunity emerged for the comprehension of the electron (or charge) transport in the nano-dimension. In fact, molecular electronic opened several questions that would not otherwise have been possible without it. Examples of it, is how it helped (and will continue doing it) to understand the electron transport phenomenology involved on important chemical and biological processes on a single-molecule basis.^{5,6}

As an introductory example of Molecular Electronics' potential, despite is a new emerging field, it helped to improve others far from its initial proposal faced to develop more efficient electronic devices, because thanks to the new achieved techniques aimed to design the molecular testing-benches as extremely accurate molecular trapping and detection systems, they helped to the molecular recognition field, because such techniques contributes with their high precision, to improve any system designed to read the chemical information of a single molecule electronically,⁷ which opens the door to very efficient chemical and bio-sensor applications based on the electrical detection of individual molecular binding events.^{8,9}

...But, how did everything start?...

1.1.1 A story of circuits and molecules...

Technology under Moore's law

In 1965, the co-founder of Intel, Gordon E. Moore, predicted that the density or number of transistors on a single integrated circuit chip roughly doubles every 18 months (see Figure 1.1 left panel).¹⁰ This increase in transistor density leads to an exponential growth in computing power.^{10,11} Therefore, Moore's law represents the driving force of progress in technological and consequent in information, communications society or even economic change in the late 20th and early 21st centuries.¹¹⁻¹³ The law is used in industry based on semiconductor and others key computer components, such as the DRAM memory, as a guide long-term planning and to set targets for research and development.¹¹ Unfortunately, microelectronics industry roadmaps expect to be able to reach the 5 nm technology limit to soon. Beyond this limit, known as Moore's limit (see Figure 1.1 left panel), the quantum nature of atoms and molecules is foreseen to determine increasingly the behavior of those components.

But, for what reason we need smaller devices, year after year? Because the demand for increasing working power can only be achieved by a parallel increase in the number of individual elements in a single chip, but maintaining its size (see Figure 1.1 right panel). Nowadays, a chip with an area of 1 cm^2 comprises a number of transistors of 10^9 order. This is achieved by decreasing the size of these elements. Indeed, the length of the channel that joins the source and the drain in a transistor is used to name the technology generation of a chip. In fact, current leading edge chips use the 14 nm (*Kaby Lake*) technology, designed by Intel in Israel and released by the end of 2016.

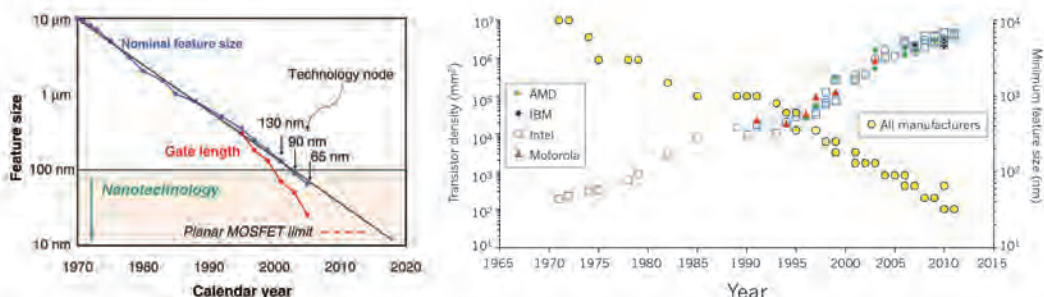


Figure 1.1: (Left) Logic technology node and transistor gate length versus calendar year. Adapted from Thompson et.al.¹¹ (Right) The evolution of transistor density (left axis) in microprocessors and gate length (minimum feature size) over time (right axis). Adapted from Ferain et. al.¹⁴

In summary, current technology is reaching its physical limits, and its due different of reasons. The most repetitive is the drawing resolution of the optical lithography used to produce the present Field Effect Transistors (FETs) (see Figure 1.2 bottom panel), which is about 0.4-0.7 micrometers due the wavelength of visible

light.¹⁵ Despite can be decreased improving the technique (is calculated a reduction until to 0.2 micrometers)¹⁶ or replacing it by others lithographic techniques such as X-ray or electron-beam lithography with an expected improvement of the resolution about 50 nm,¹⁶ it will not represent a substantial long term solution. Also, exist drawbacks associated to specifically to a device, for example to the DRAMs. To downscale their capacitors, is required a reduction in the thickness of the dielectric spacer, currently at about 1 nanometer, but this value represents a physical barrier since electric fields generated *in-situ* are larger than the maximum field that they can withstand (107 V/cm). Also, current FETs present power lost due the leakage of currents between the gate and the drain regions. Since the oxide layer is used to separate the gate and the channel barrier (see Figure 1.2 left right), if it becomes thinner, the electrons can tunnel from one side to the other at an ever-increasing rate. As a consequence, is generated heat management problem as well as an impaired signal to noise ratio and also it impossibilities the controlled gate electrodes.

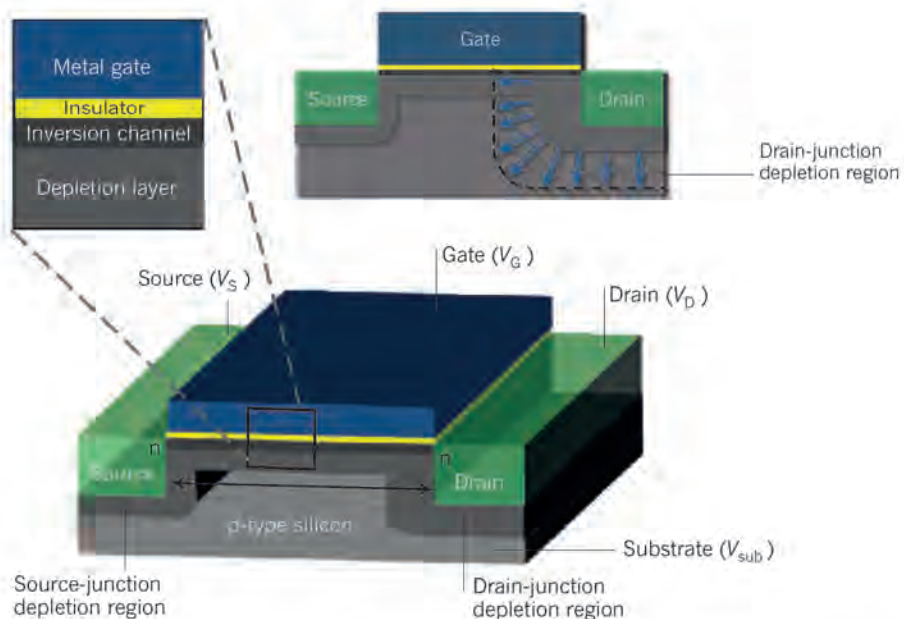


Figure 1.2: A schematic view of a classical bulk n-channel MOSFET. Two n-type regions called the source and the drain are formed on a p-type substrate. These regions are separated by a distance L , which is called the channel length. A gate stack (insets) composed of an insulator and a metal gate electrode is placed above the p-type substrate between the source and the drain. When a positive bias (or positive voltage) is applied to the gate, electrons from the source and the drain are attracted by the gate and form an inversion layer, which is called the channel, which connects the source to the drain. Holes in the substrate are repelled by the gate and absorbed by the source and the drain in the vicinity of the junctions, creating hole-starved regions, which are called depletion regions. V_G , gate voltage; V_S , source voltage; V_{sub} , substrate voltage. (Right inset) The width of the drain-junction depletion region increases (depicted with blue arrows) as the drain voltage (V_D) increases, causing the drain-induced barrier lowering effect. Adapted from Ferain et al.¹⁴

Exist three alternatives^{11,17} to overcome Moore's limit:

1. “*More Moore approach*”: Is based on decreasing the size of the electronic components, and also looks for more efficient electronic components and better system architectures (disposition of the components inside a board or electrical device).
2. “*More than Moore approach*”: Challenge for the gradual integration of new components, aiming to add new to the current CMOS technology.
3. “*Beyond Moore approach*”: includes a new absolute vision of the building blocks to develop any device based on electronics, because proposes replace electronic devices by atoms or molecules. Such paradigm change not only involves absolute new system architectures but also will push the replacement of the *Boolean* logic by more efficient algorithms, possibly based on quantum computation.

In summary, Molecular Electronics represents the paradigm of the *Beyond Moore approach*. But despite experimentally is a very recent field, to explain the beginnings of Molecular Electronics we, have to go back to 1950s in the middle of the cold war...

Technology perspectives *Beyond Moore's law*

In 1956, Arthur von Hippel stated the need of bottom-up approach in Molecular Electronics,¹⁸ which he named molecular engineering. In 1958, the company Westinghouse and US Air Force created a program where von Hippel's ideas were tested.^{12,13} The US Air Force organized a conference on Molecular Electronics, in which it was, probably, the first time that this term was used in public. There, Colonel C. H. Lewis, director of the Electronics program at the Air Research and Development Command, presented the Molecular Electronics as the next step in electronics. A few years after this congress, experimental studies on this field were abandoned.¹² The breakthrough for the Molecular Electronics field, was in the late 60's and early 70's, the studies of the modern Molecular Electronics we know today began.^{12,13} Different groups started to investigate the electronic transport through molecular monolayers. Hans Khun and coworkers at Gottingen University and Ari Aviram at IBM company are prominent examples. Khun and coworkers exploited Langmuir-Blodgett films to experimentally study transport through a monolayer, while Aviram at IBM began working on the theory of electron transfer through a single organic molecule in collaboration with Mark Ratner. In 1974, Aviram and Ratner³ published their nowadays famous paper on “molecular rectifiers” (explained on Figure 1.3), that is probably the first proposal to use a single molecule as an electronic component.

At the end of the 1970's and the beginning of 1980's, other investigators started to work on similar ideas to Aviram and Ratner.^{3,12,13} Forrest Carter, a chemist at

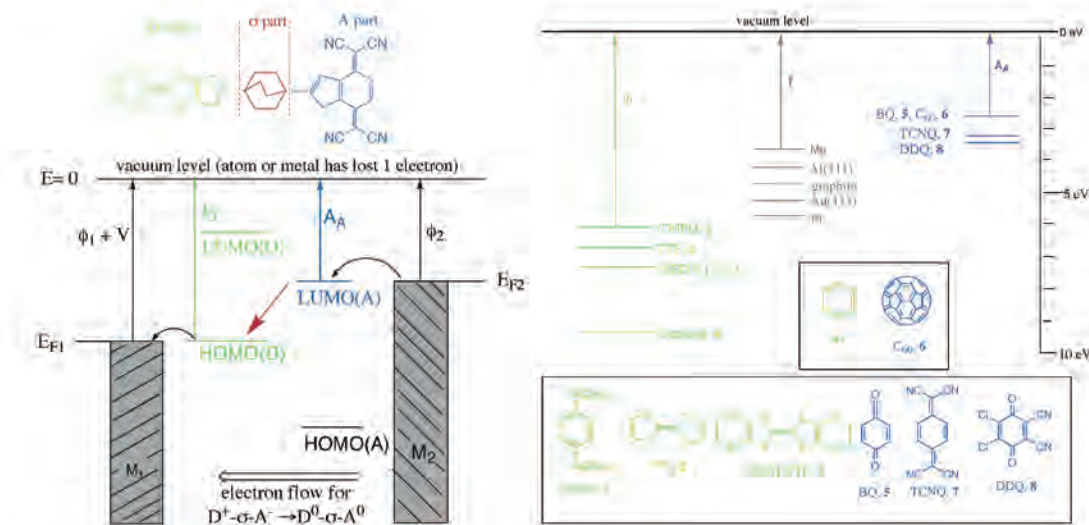


Figure 1.3: (Top) Ideal ($D-\sigma-A$ to) single-molecule rectifier (which was never synthesized). (Bottom) Diagram for the electron transport through the molecule flowing from the excited zwitterion state $D^+-\sigma-A^-$ to the undissociated ground state $D^0-\sigma-A^0$, when the molecule is placed between two metal electrodes M_1 and M_2 . Here $E=0$ is the vacuum level, ϕ is the work function of the metal electrodes, V is the potential applied on the left electrode (the right electrode is grounded), I_D is the ionization potential of the donor moiety D , A_A is the electron affinity of the acceptor moiety A , and E_{F1} and E_{F2} are the Fermi levels of the metal electrodes, the HOMO and LUMO levels refers to frontier orbitals orbitals of the D and A moieties. Adapted from Metzger.¹⁹

the Naval Research Laboratory, was able to create the first community of Molecular Electronics and organized a series of conferences the 1980s, gathering the researcher from very different disciplines. These conferences had an important role in the history of this area. The scene of Molecular Electronics had an important change in 1981 when Gerard Binnig and Heinrich Rohrer invented the STM,²⁰ allowed handling and observing matter at the atomic scale and confirmed Khun's and Aviram's theories molecular electronic approaches are inherently digital, and some of them are inherently nonvolatile.

...Previously to the design of any applied technology based in single-molecule electronic devices, was (and still it is) needed understand the phenomenology of a junction at the nano-scale. The following sections aims to summarize the most elemental concepts...

1.1.2 Electron Transport in Nanoscale Junctions

The best way to explain the electron transport through a junction at the nanoscale is via the analogy to the bulk scale, where Conductance (G) in wire-like conductors follows the well-known Ohm's Law (*Expression 1.1*) and is proportional to its cross-section area (A) but proportional to its length (L):

$$G = \sigma \frac{A}{L}, \quad (1.1)$$

σ is the specific electrical conductivity of a material and it depends on its intrinsic properties and does not show any dependence on L or the diameter of the wire. However, if the dimensions of the conductor length (L_c) decreases in some orders of magnitude and the current is flowing through atomic-size or molecular-size conductors some concepts like Ohm's law are not applicable. In fact, conductors in the nanoscale represent the limiting case for mesoscopic systems in which quantum coherence plays a essential role in the transport properties, being one of the fundamental reasons of Moore's law limits as is explained on *Section "Technology under Moore's law"* (Page 3).

In order to understand the transition from the classical to the quantum regimes and according to the relative size of various length scales, different transport regimes can be identified, which in turn, are determined by different scattering mechanisms.²¹

- **Phase-coherence length** or **phase-relaxation length** (L_φ): length over which quantum coherence (*phase*) of an electron wave is preserved. If the sample L is smaller than L_φ , the electron waves interfere with each other and phase coherence can be destroyed. Such interferences are mainly inelastic scattering mechanisms due electron-electron and electron-phonon interactions as well as scattering of electrons by magnetic impurities, with some internal degrees of freedom, also degrades the phase, unlike the elastic scattering by (static) non-magnetic impurities which does not affect the coherence length.
- **Elastic mean free path** or **momentum-relaxation length** (L_m): measure of the distance between elastic collisions with static impurities, i.e. the average distance where an electron can travel before its collision with any impurity or defect in the conductor.

Assuming an elastic scattering, in which the electron does not lose or gain energy, the electron can change its momentum but not its wave coherence. Therefore, elastic scattering contributes to L_m but not to the L_φ . However, the inelastic scattering contributes to both L_m and L_φ . Using the above explained characteristic lengths, the electron transport can divided into the following *ballistic*, *diffusive* and *classical regimes*:^{21,22}

1. **Classical Transport** ($L_c >> L_m >> L_\varphi$): The electron wave experiences scattering events during the transport through the conductor. The electron wave

is not coherent, thus electron wave interference can be neglected. Assuming a classical transport regime model and considering the electron as a particle with a uniform distribution of the scattering centers along the conductor the effective resistance is proportional to the length L_c , therefore and Ohm's law is valid.

2. **Diffusive transport ($L_c > L_\varphi \gg L_m$)**: The electron wave loses momentum information but remains coherent. This case involves many elastic scattering events which lead to change the electron momentum but not in wave coherence (see Figure 1.4 left panel).
3. **Ballistic transport ($L_c \ll L_m$ and L_φ)**: The electron wave propagates through the conductor without experiencing any scattering event which may lead to changes in momentum or phase, thus the electron momentum can be assumed to be constant and only limited by scattering with the boundaries of the sample (see Figure 1.4 right panel). Under this scenario, G is quantized and follows the Landauer formalism (concept explained above).

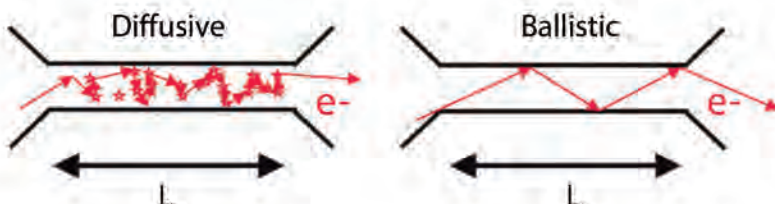


Figure 1.4: (Left) Schematic representation of diffusive transport versus (right) ballistic transport. Adapted from Rutherford et al.²³

In the previous discussion have been assumed that the effective dimensions of the sample are much larger than the *Fermi wavelength* λ_F . Since the focus of this thesis is the conduction through molecules and now we are talking about nanocontacts, such assumption can not be taken. In atomic-scale junctions the contact width (W) is of the order of a few nanometers or even less, therefore $W \approx \lambda_F$ and it implies that the conduction cannot be described by such semi-classical arguments because the dimensionality enters into the full quantum limit. The understating (form a theoretical point of view) of the G on an atomic-scale, deriving it from microscopic principles, represents a challenge for the theory. however, different models have been discussed,^{21,22} being the most representatives the Sharvin's semi-classical approximation²⁴ and the Landauer formalism.²⁵

In classical transport, the current passing through a conductor that is submitted to a voltage drop depends on the conductivity of the material and on its geometry, as described by *Expression 1.1*. Therefore a metallic wire to scale as R^2 , where R is its radius, and following the scaling law already studied by Maxwell,^{26,27} the G of a diffusive constriction, where the contact R is large compared to the L_m , is

$$G = 2R\sigma, \quad (1.2)$$

where σ scales linearly with the contact radius. If the dimensions of a conductor are much smaller than their mean free path ($L_c \ll L_m$), the electron will be transported under the ballistic regime. In such case, there will be a large potential gradient near the contact causing the electrons to accelerate within a short distance.

In 1965 Sharvin²⁴ treat the propagation of the electrical current through a ballistic contact as an analogy to the a *classical* problem of a dilute gas flow through an (small) orifice. He reasoned that if the potential difference between the two half-spaces is eV , the transported electrons through the orifice should change their velocity by the amount $\Delta v = \pm eV/p_F$, where p_F is the Fermi momentum.²⁸ The net current will be $I = ne\Delta v S$, where $S = \pi R^2$ is the contact area and taking into account the Fermi-Dirac statistics for electrons, $n = 4\pi p_F^3/(3h^3)$, the conductance for a circular ballistic point-contact is:

$$G = \frac{1}{V} = \frac{2e^2}{h} \left(\frac{\pi}{\lambda_F} \right)^2 = \frac{2e^2}{h} \left(\frac{k_F R}{2} \right)^2, \quad (1.3)$$

where e is the electron charge, h is Planck constant and k_F is the Fermi wave vector. Notice that according to Shaik's argument, G is proportional to the contact area, like in Ohm's law, but the proportionality constant $2e^2/h$ has a quantum nature. Also such G , unlike Ohm's law, is totally independent of σ as well as L of the G channel and is determined only by its cross-section radius R .

Although *Sharvin's G* formula describes well the G of ballistic contacts (mesoscopic conductors) with diameters down to a few nanometers, it cannot explain the G of a nanoconductor consisting of only a few or a single atom at the constriction. As a complementary correction can be used so-called Weyl correction to *Expression 1.3*. This correction comes from the fact that Heisenberg uncertainty principle for Fermi electrons in a narrow contact, $2p_F R \geq \hbar$, provides a small correction to the *Sharvin's G* as follows in *Expression 1.4*, but only is valid for atomic contact in the form of a wire.

$$G = \frac{1}{V} = \frac{2e^2}{h} \left(\frac{k_F R}{2} \right)^2 \left(1 - \frac{2}{k_F R} + \dots \right). \quad (1.4)$$

Due to the limitations of the semi-classical approaches of *Expressions 1.3 and 1.4* which do not account for purely quantum effects which dominate the transport when employing contact size so small the wave nature of an electron can no longer be ignored. For such reason Rolf Landauer from *Thomas J. Watson IBM Research Center* devised the treatment of current flow as transmission process based on a scattering approach, known as the *Landauer formalism*.^{25,29}

First of all, should be understood the total G as transmission, as proposed Landauer and summarized mathematically on his famous *Landauer formula* (*Expression 1.5*). To obtain it, Schrödinger equation has to be solved as well as the current-carrying eigenmodes found to calculate their transmission values and sum up their contributions.^{21,22} For such reason *Expression 1.5* contains the summation of all the

available conduction modes introduced to the equation through, T_n which is each individual transmission.

$$G = \frac{1}{V} = \frac{2e^2}{h} \sum_{n=1}^N T_n. \quad (1.5)$$

As is deduced from 1.5, if T_n of a mode is perfect (equal to 1), contributes exactly one quantum unit of conductance ($G_0 = 2e^2/h \sim 77,49 \mu\text{S}$), scenario known as conductance quantization. This formula shows that by changing the size of the contact, one can change the number of modes contributing to the conductance and thus the conductance itself in a step-like manner

The deduction of the Landauer formalisms (*Expression 1.6*) along with its discussion does not represent the aim of this chapter neither this thesis since is a well-known development based on an heuristic argument.^{21, 22, 25, 29} Nevertheless, some qualitative points should be clarified. The basic idea of the scattering approach is to relate the transport properties to the transmission and reflection probabilities for charge carriers (the electrons) passing through the conductor as the central part of the junction established between two metal leads, and is based in two assumptions:

1. In this one-electron approach, phase-coherence is assumed to be preserved in the course of electron transport through the conductor, as well as inelastic scattering is restricted to the macroscopic leads or electrodes which behaves as ideal electron reservoirs (*place where the electrons are inside*) in thermal equilibrium with a well-defined temperature and chemical potential.²¹ Therefore, such reservoirs enter into the description as a set of boundary conditions instead of dealing with complex processes occurring inside the reservoirs.
2. The other assumption is based on taking the conductor as the only *place* where scattering happens. And is characterized by a transmission function $T(E)$. The best way to understand it is defining that such conductor as a (one-dimensional) potential barrier of length L affected by a wave-function (plane wave), $(1/\sqrt{L})e^{ikx}$ which is partially reflected (loses energy) with a probability amplitude r and partially transmitted with a probability $T=|t|^2$, as Figure 1.5 tries to represent.

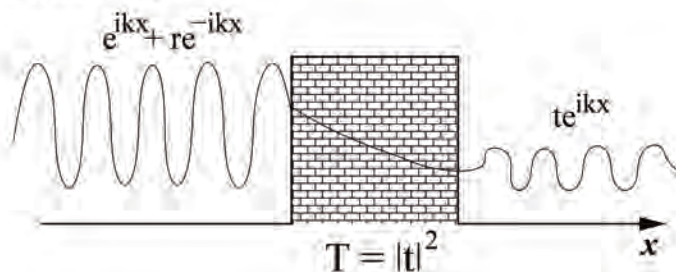


Figure 1.5: Plane wave impinging on a one-dimensional potential barrier. The wave is partially reflected with a probability amplitude (r) and partially transmitted with a probability ($T=|t|^2$).

Thanks to the explained formalism the total current following through a junction between two electrodes with a established electrical potential difference can be treated as the follows expression 1.6 which represents the simplest version of the so-called Landauer formula, but it illustrates perfectly the close relation between current and transmission (is important highlight the extra factor 2 to account for the spin degeneracy):

$$I(V) = \frac{2e}{h} \int_{-\infty}^{\infty} dE T(E) [f_L(E) - f_R(E)]. \quad (1.6)$$

From Expression 1.6 can be deduced that at zero temperature $f_L(E)$ and $f_R(E)$ are step functions, equal to 1 below $\varepsilon_F + \frac{eV}{2}$ and $\varepsilon_F - \frac{eV}{2}$, respectively, and 0 above this energy. If also low voltages are assumed (*linear regime*), this expression is simplified to $I = G \cdot V$, where $G = \frac{2e^2}{h} T$ and the transmission is evaluated at the Fermi energy(ε_F). This simple calculation demonstrates that a perfect single mode conductor between two electrodes has a finite resistance, given by the previously commented universal G_0 , also known as *Landauer Conductance*. This is a useful magnitude as can be used to detect quantum contacts with any platform which allows the formation of nano or molecular junctions, and represents a common and very used reference to express any measured conductance. This is an important difference with respect to macroscopic leads, where one expects to have zero resistance for the perfectly conducting case. The proper interpretation of this result was first pointed out by Imry,³⁰ who associated the finite resistance with the resistance arising at the interfaces between the leads and the sample.

The Landauer approach, holds well for typical Molecular Electronics transport experiments or nanoscale devices, which consist in connect (*trap*) a molecule or a sample between two macroscopic electrodes which inject currents at fixed voltages. Undoubtedly, transmission probability plays a central role and it is worth reminding how this quantum mechanical quantity can be computed in some simple situations of special interest like single potential barriers. This simple problem not only illustrates some fundamental issues, but it also provides a basic model widely used for the understanding of tunneling currents in a great variety of situations such as tunnel junctions based on insulating barriers, STM and even single-molecule junctions, the main focus of interest for this thesis. The description of tunneling transport through a molecule in its associated *molecular barrier* is not an easy task. Several effects should be taken in account, such as as the hybridization of the molecular states with the metals or interfacial dipoles. Examples of a huge variety of factors which play a role on the (molecular) barrier potential shape making its modelization significant difficult. In fact, many decades after the establishment of the Molecular Electronics field, the precise contribution of all these effects to the transport is still unclear and despite different approaches have been proposed, the satisfactory description of these systems still represents an open challenge. Even so, exist two well extended models to use. The (*i*) Simmons model³¹ and the (*ii*) Tunneling transport through

the molecule. The former comes from the community of solid state physics, and represents a sort of adaptation of the existing approaches to describe tunneling transport phenomena of metallic tunnel junctions and semiconducting inorganic devices. Represents one of the first models that describes tunnel transport through thin insulating films, thus the adequacy of adapting this model to the description of metal-molecule-metal contacts is controverted. For this reason the other possible model, coming from chemistry community, incorporates the molecular features right from the start to describe these electron transport at the single-molecule level.

1.1.2.1 The Simmons Model

The Simmons model was introduced in 1963 to describe the electron transport between metallic electrodes through a thin insulating film under a tunneling mechanism.³¹ This approach adopts a non-interacting free electron approximation employing the developed one by Wentzel-Kramers-Brillouin. In such model the tunneling current presents dependence on the mean value of the barrier height ($\bar{\varphi}$), but can be applied the simplification of the problem of a potential barrier of arbitrary shape to a rectangular one.³¹ According to the described, the *zero-temperature* net (tunneling) current density (J) through a generalized barrier can be expressed as:

$$J = J_0 \{ \bar{\varphi} e^{-A\sqrt{\bar{\varphi}}} - (\bar{\varphi} + eV) e^{-A\sqrt{\bar{\varphi}+eV}} \}, \quad (1.7)$$

if

$$J_0 = \frac{e}{2\pi h(\xi\Delta s)^2} \quad (1.8)$$

and

$$A = \frac{4\pi\xi\Delta s\sqrt{2m_e}}{h}, \quad (1.9)$$

where Δs is the barrier width at the ε_F of the electrodes, m_e is the free electron mass, V is the applied voltage and h is the Planck constant. Moreover the term ξ is the dimensionless correction parameter correction factor of order unity for $V > \bar{\varphi}/e$. It is possible to simplify the general equation (in this text *Expression 1.7*) to the case of a rectangular barrier if we consider $\bar{\varphi} = \bar{\varphi}_0$, where $\bar{\varphi}_0$ is the height of the rectangular barrier and $\Delta s = s$ is the thickness of the insulating layer and can be approximated in three distinct cases depending on the applied voltage ranges summarized on Figure 1.6.

- 1. Low-Voltage Ranges (Figure 1.6 a):** For very small V ($eV \sim 0$) $\bar{\varphi}$ can be assumed as independent parameter respect to the V and $\bar{\varphi}_0 = (\frac{\bar{\varphi}_1+\bar{\varphi}_2}{2})$ obtaining the following expression:

$$J = J_L V; J_L = \frac{e^2 \sqrt{2m_e \bar{\varphi}}}{4\pi^2 \xi \hbar^2 \Delta s} e^{-A\sqrt{\bar{\varphi}}}. \quad (1.10)$$

2. Intermediate-Voltage Ranges (Figure 1.6 b): For medium applied V ($eV < \bar{\varphi}$) is defined by $\frac{\bar{\varphi}_1 + \bar{\varphi}_2 - eV}{2}$. Besides, J can then be simplified assuming that $\Delta s = 1$, obtaining the following expression:

$$J = J_L(V + \gamma V^3); \gamma = \frac{(Ae)^2}{96\bar{\varphi}_0} - \frac{Ae^2}{32\bar{\varphi}_0^{3/2}}. \quad (1.11)$$

This expression results useful to determine both the $\bar{\varphi}$ and Δs in terms of the coefficients γ and J_L .

3. High-Voltage Ranges (Figure 1.6 c): Under scenarios when $eV > \bar{\varphi}$, $\bar{\varphi}$ is reduced to $\bar{\varphi}_1/2$ and even Δs is also reduced. If the applied V is high enough so that the ε_F of Electrode₂ is lower than the G band of Electrode₁. In this case, tunneling from Electrode₂ in Electrode₁ is not possible since there are no empty states in Electrode₁ to tunnel to. As for electrons tunneling from Electrode₁ into Electrode₂, all states in Electrode₂ are empty. This is analog to field emission from a metal into vacuum. Thus the J can be simplified as the following with the electric field strength in the insulator $F = V/s$, where s is the thickness of the insulating field:

$$J = \frac{2.2e^3}{8\pi h} \cdot \frac{F^2}{\bar{\varphi}_1} e^{-\frac{8\pi\sqrt{2m}\bar{\varphi}_1^{3/2}}{2.96e\hbar F}}. \quad (1.12)$$

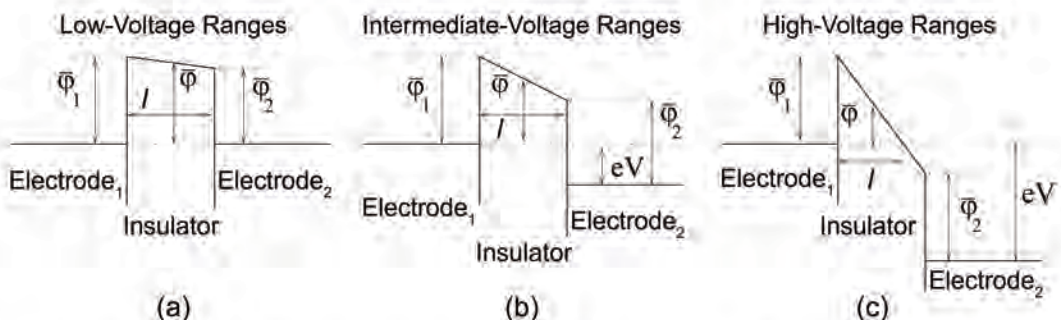


Figure 1.6: Tunneling through a junction in which two metallic electrodes (Electrode₁ and Electrode₂) are separated by a thin insulating film (insulator in the figure), which is modeled as a rectangular potential barrier. The three panels show the three distinct voltage ranges discussed in the text (a) Low-Voltage Ranges, (b) Intermediate-Voltage Ranges and (c) High-Voltage Ranges. Adapted from Cuevas.²¹

Despite the Simmons model suffered adaptations quite popular in Molecular Electronics field, represents a model originally designed for being used for inorganic materials, therefore is quite questionable since molecules present discrete levels instead of a continuum of states, which produces hybridization and coupling effects that are not taken into account on the potential barrier. For this reason, other approaches coming from the chemistry community like the explained at follows, are

more adequate since incorporate the required molecular features from the beginning, although in some cases still use some concepts provided by Simmon's model.

1.1.2.2 Transport Mechanisms in Molecular Junctions

Several transport mechanisms in molecular junctions have been proposed and studied, among them the most extended are the following different mechanisms: *Direct tunneling*, *Fowler-Nordheim tunneling*, *Thermionic emission* and *Hopping conduction*, summarized in the following *Table 1.1* and explained above:

| Conduction mechanism | Characteristic behavior | Temperature | Voltage dependence |
|----------------------------------|--|---------------------------------------|---------------------------------------|
| <i>Direct tunneling</i> | $J \sim V e^{-\frac{2L}{\hbar} \sqrt{2m\varphi}}$ | none | $J \sim V$ |
| <i>Fowler-Nordheim tunneling</i> | $J \sim V^2 e^{-\frac{2L\sqrt{2m\varphi^3}}{3q\hbar V}}$ | none | $\ln(\frac{J}{V^2}) \sim \frac{1}{V}$ |
| <i>Thermionic emission</i> | $J \sim T^2 e^{-\frac{\varphi - \sqrt{2m}}{K_B T}}$ | $\ln(\frac{J}{T^2}) \sim \frac{1}{T}$ | $\ln(J) \sim V^{1/2}$ |
| <i>Hopping conduction</i> | $J \sim V e^{-\frac{\varphi}{K_B T}}$ | $\ln(\frac{J}{V}) \sim \frac{1}{T}$ | $J \sim V$ |

Table 1.1: Possible conduction mechanisms. Here, J is the current density, V is the bias voltage, L is the barrier length, φ is the barrier height and T the temperature.

Direct tunneling and *Fowler-Nordheim tunneling*, in fact are two manifestations (regimes, to be more precise) of the coherent tunneling mechanism through a rectangular potential barrier and are based on the Simmons model previously explained (see Page 12). They present dependence on temperature and voltage. Regarding voltage and its use on the mentioned Simmons model, in this case also determines the application of both regimes, then the direct tunneling refers to what happens under at low bias regimes, typical of single-molecule conductance measurements because the voltage is much smaller than the barrier height; and contrary, whereas Fowler-Nordheim tunneling occurs when voltage is larger than the average barrier height and it is similar to field emission. Both scenarios have in common that the $I(V)$'s are rather insensitive to temperature and they only differ in the voltage dependence.

The third mechanism, the *thermionic emission*, is a process that takes place when the electrons are excited over a potential barrier, oppositely to tunneling through it. As is deductible it has a clearly strong dependence on temperature, which becomes significant when the potential barrier is relatively small. In fact, according to the theory²¹ thermionic emission is also a coherent mechanism since the electrons proceed elastically through the barrier without losing phase memory (see Page 7).

Finally, *hopping conduction* is a mechanism in which the injected electron is localized at certain points within the molecule, and hopes between those points and also is a thermally activated process. Such mechanism dominates the transport properties of long molecules like DNA,^{32,33} except in some exceptional cases such as

CNT which is resonant tunneling mechanism (scenario explained further below).

Regarding the thermal activation concept and its involvement on the conduction mechanisms, they can be classified in two distinct categories: (*i*) thermionic or hopping conduction which has temperature-dependent I(V) characteristics, and (*ii*) both coherent tunneling mechanism regimes (direct tunneling and Fowler-Nordheim tunneling), which does not exhibit temperature dependent I(V) curves. According to that, an easy way to elucidate the transport mechanism is to perform conductance measurements under a variable working temperature, allowing to classify the dominant conduction mechanism according the observed temperature-dependent behavior.

From the above all the briefly explained transport mechanism, *coherent tunneling* and *incoherent hopping* mechanisms are the most extensively used in single molecular junctions, for this reason they are detailed discussed on the next sections:

Coherent Tunneling Mechanism

As was explained previously, the *coherent (non-resonant) tunneling* process defines an electron transport through molecules under an electron tunneling through a rectangular (molecular) barrier which does not depend on temperature, but decays exponentially according the molecular length (l) (see *Expression 1.16*).

In a coherent tunneling process the electron has a ballistic behavior (see Page 7), and regarding the *Landauer Formalism*, is assumed that the scattering happens at both the metal-molecule interface as well as along the molecular wire itself, therefore the electron transmission comprises the contribution of the analogous three components^{30,34} (see *Expression 1.13*) to the associated efficiency of the electron transport through the molecule T_M and across the left or the right metal-molecule, T_{LC} and T_{LR} respectively, as is summarized below:

$$T = T_{LC} \cdot T_M \cdot T_{LR}. \quad (1.13)$$

Since in the junction, the molecule is considered a rectangular tunneling barrier,^{21,30,34,35} therefore:

$$T_M = e^{-\beta l}, \quad (1.14)$$

employing Landauer's dependence between and G and transmission, the effective conductance can be expressed as

$$G(l) = A \cdot e^{-\beta l}, \quad (1.15)$$

since A parameter is a prefactor that determines the order of magnitude of the conductance and using the *Landauer Conductance notation*, can be obtained the widely used expression for the effective molecular conductance:

$$G_M = G_0 \cdot e^{-\beta l}. \quad (1.16)$$

Expression 1.16 and the previous *Expression 1.15*, clearly show how G decays exponentially with the length of the molecule (l) as well as on the β parameter, the tunneling decay on length:

$$\beta = 2 \sqrt{\frac{8\pi^2 m^* \alpha [\bar{\varphi} - \frac{eV}{2}]}{h^2}} \quad (1.17)$$

where h is the Planck constant, m^* is the effective electron mass ($0.16 m_0$), V is the applied bias voltage between the electrodes, α is a common employed parameter aimed to describe the asymmetry in the potential profile across the junction ($\alpha = 1$ under symmetric molecule's coupling with the electrode) and $\bar{\varphi}$ is the barrier height, which in this context is the barrier through the HOMO or LUMO level, $\bar{\varphi} = \varepsilon_F - E_{HOMO}$ or $\bar{\varphi} = E_{LUMO} - \varepsilon_F$ respectively.

Similarly to the calculated for G_M , the effective contact resistance can be calculated as follows:

$$G_C = G_0 \cdot T_{LC} \cdot T_{RC} = G_0 \cdot T_{Contact}, \quad (1.18)$$

for this reason, if any frontier orbital (HOMO or LUMO) is aligned with the ε_F , (coherent) resonant tunneling occurs, thus $\bar{\varphi} = \frac{eV}{2}$ and consequently $\beta = 0$. Under this scenario G is fully dominated by the contacts between the electrodes and the molecule, which increases the number of conducting modes and is independent of the molecular length. This scenario can occur if are employed large conjugated systems like graphene or CNTs, which despite being large and intuitively related to hopping mechanisms, show such coherent resonance.^{21,22,36}

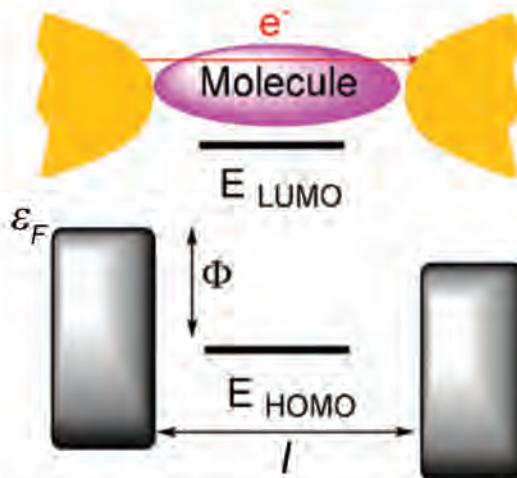


Figure 1.7: Schematic representation of coherent tunneling mechanism through a molecular junction. Here the HOMO level is closer to ε_F as LUMO level. The barrier height is given by $\bar{\varphi} = \varepsilon_F - E_{HOMO}$. If the LUMO is closer to ε_F , one obtains accordingly for the barrier height $\bar{\varphi} = E_{LUMO} - \varepsilon_F$. l represents the width of the barrier (molecular length). Adapted from Rigaut et al.³⁷

Incoherent Hopping Mechanism

The *incoherent hopping mechanism*^{21,22} (Represented as a cartoon on Figure 1.8) involves series of transfers between relatively stable states. It happens when the *transport time* is comparable to the time scale of any motion in the environment surrounding the molecule and the consequent inelastic events play a dominant role in the electron transport. Since the thermal (nuclear) motion of the electron transfer does not occur until it is achieved a favorable molecular geometry, the hopping mechanism involves the electron motion over a barrier. Such nuclear motion represents the main difference between hopping and tunneling, and it can be understood like the molecule and/or its environment need to be rearranged in a certain way for electron transfer to occur, while tunneling involves electron transfer through the barrier, i.e. exists a finite probability of finding an electron on the other side of the barrier, without the nuclear motion requirement.

Hopping mechanism is characterized by an inverse proportionality of the molecular conductance, respect the (molecular) length and temperature (mentioned before in *Table 1.1*, on Page 14). Regarding the former, this mechanism follows a linear behavior, but respect the temperature, follows an exponential behavior ($e^{\frac{-\Delta E}{k_B T}}$, where $-\Delta E$ is the activation energy of the target system).

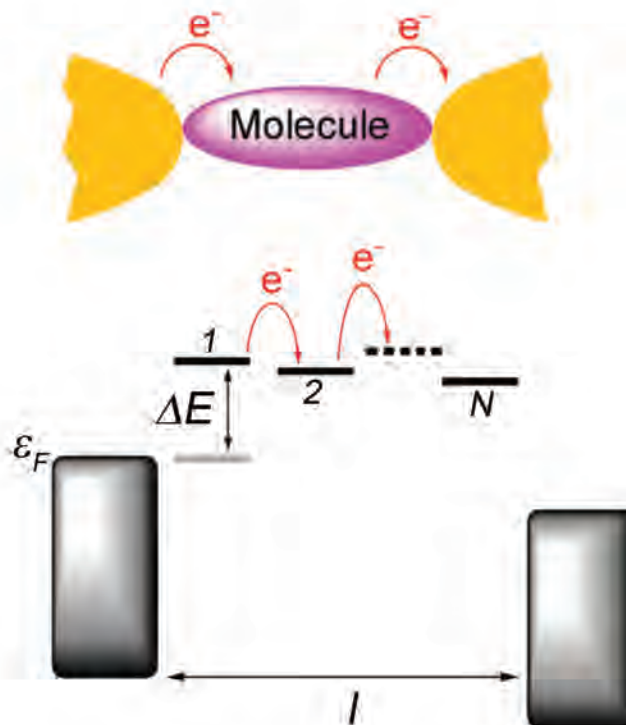


Figure 1.8: Schematic representation of incoherent hopping mechanism through a molecular junction. $-\Delta E$ is the activation energy, l represents the width of the barrier (molecular length) and (N) the number of bridge levels. Adapted from Rigaut et al.³⁷

Hopping mechanism is typically observed for electron transfers carried out on long molecular wires associated to a high number of bridge levels (N) and low activation energies ΔE , two concepts combined to define a very useful magnitude, the *tunneling traversal time* (τ),^{21,30,34,35} which can be defined as the residence time of an electron “*inside the junction*”, thus hopping mechanisms present higher values than coherent tunneling mechanism:

$$\tau \approx \frac{N\hbar}{\Delta E}, \quad (1.19)$$

In general, can be assumed that for short molecules, (i.e. small N and high ΔE), the transmission is dominated by a tunneling mechanisms (shorter τ), while for long molecules (with high N and small ΔE) the transmission is dominated by an hopping mechanism (longer traversal time). To distinguish between these two mechanisms experimentally, as was proposed before one has to investigate the as temperature dependencies of the molecular conductance.

1.1.3 *Beyond than Moore*: Molecules as electronic components

Finding realistic ways to build effective molecular-based junctions which behave as conventional electronic circuit components represents a fascinating challenge. Thus, the scientific interest in understanding electronic transport via molecules is significant. The main focus a part form the fundamental point of view, are the fabrication methods and ensemble's stability. At the next sections are summarized the advantages of the Molecular Electronics in front the conventional electronics and the main features to control:³⁸

Advantages of Molecular Electronics

- **Size:** Thanks size scales between 1 and 100 nm of molecules, Molecular Electronics represents the torchbearer of the Beyond Moore discipline for the electronics future.
- **Tailorability:** Thanks to the development in chemical synthesis, the molecular design is a very accessible tool which entails overcoming formidable obstacles, e.g. allows getting of molecules with a broad variety of functionalities which can adapt to any specification, also can be used several synthetic strategies to improve the molecular attachment with the electrodes thus enhancing the long-term stability and even to increase the molecular capabilities, allowing to the molecules exhibit multiple functionalities and applications.
- **Self-assembly and recognition:** Selective molecular interactions help to form complex structures by self-assembly with extraordinary precision and reproducibility.
- **Computational support:** Thanks to the advances of computational science, the behavior as well as capabilities of the molecular systems can be previously simulated. Combined with synthesis, they lead to the best molecular design to achieve specific electronic functionalities.
- **Suitable for digital information:** Many of the molecular electronic approaches are inherently digital, and some of them are inherently nonvolatile.

Significant molecular features

Molecules as functional blocks can offer thousands of capabilities, but also, they must not only have the desired properties, but also have proper other features which guaranties the functionality as building blocks. Below are detailed the most significant features studied to the date, which can affect the electron transport through molecules:

- **Molecular Structure:** Represents the basic property and can be used to tune the junction conductance in different ways, for this reason is the most modified

molecular factor, and therefore all the possibilities cannot be summarized. But at least, the most studied cases can be generalized as follows. Modifications on the chemical substituents are essential,^{39,40} for example they can affect to the molecular conductance, as consequence of their electron-donating or electron-withdrawing capabilities;⁴¹ the molecular symmetry also is remarkable, since can affect to the molecular orbital phases,⁴² or when is broken, can cause current rectification effects; another example can be the molecule's degree of conjugation,⁴³ because π -orbitals enhance the molecular conductance since increase the electronic contribution to the electron-pathway.^{36,44}

- **Redox-state:** The redox state is one of the most important parameters for studying the functionality of a molecule (i.e. molecular switches or rectifiers) using electrochemical gating.⁴⁵ In 2003, Haiss et al.⁴⁶ were the first to demonstrate that single molecule conductance can be determined in an electrochemical environment. Later on, other effects have been demonstrated, as example the electrochemically controlled quantum interference phenomenon reported by Darwish⁴⁷ and colleagues, or the employment of the electrochemistry to control a transistor-like behavior and switching effects on proteins.^{48,49}
- **Linker groups:** Also, known as anchoring groups, they have to gather different specifications, such as present a low contact resistance; ensure a strong chemical and mechanical connections between a molecule and the respective leads (usually metal electrodes), and also form well-controlled and reproducible molecular junction geometries. Many anchoring groups were reported in the literature,^{50–54} the most significant are: thiol (-SH), isocyanide (-NCR), (-SO_3^-), hydroxyl (-OH), nitrile (-CN), amine (-NH₂), carboxylic acid (-COOH), benzyl (-C₆H₅), pyridyl (-C₆H₅N) or even C₆₀. In some cases, when the system allows it, the molecule can be chemically linked direct to Au-C,⁵⁵ which present a strong interaction, low resistivity contact and a strong electronic coupling. In fact, junctions formed with the prototypical molecule 1,4-dimethylenebenzene, revealed a conductance value approaching 1G_o. Junctions formed with methylene-terminated oligophenyls with two to four phenyls units showed a 100-fold increase in conductance as compared with those formed with oligophenyls of similar length but using amines as anchoring group.
- **Molecular length:** Charge transport through metal–molecule–metal junctions has been investigated by measuring the conductance as a function of molecular length, depending on the length of the molecule, are assumed two different transport mechanisms called tunneling and hopping (see *Section “Transport Mechanisms in Molecular Junctions”* on Page 14) extensively reported.⁵⁶ The transition between both mechanism also is a widely-studied issue at molecular level. Wang's team performed an interesting study of such transition employing oligo (p-phenylene ethynlenes) (OPEs) derivatives and Ferrocene oligomers.^{57,58}
- **Electrode Material:** Au represents the most used material to build electrodes because is easy to orient, present affinity for several kinds of anchoring

groups and is highly resistive to the oxidation under ambient conditions. Even so, other materials have been used. Like Pt,⁵⁹ Cu,^{60,61} Pd,⁶⁰ Fe,⁶⁰ Ag⁶¹ and very recently Si.⁶² In such studies,⁶¹ the authors claim that the decrease in conductance indicates, the weakening of electronic coupling at the electrode-molecule contacts.

- **Solvent Effect:** Since in many single-molecule techniques the conductance experiments are performed at the solid/liquid interfaces, is required the careful consideration of solvent effects. Surprisingly, only few contributions studied this issue. Li et al.⁶³ reported conductance measurements of alkanedithiol in polar ionic, and nonpolar organic solvents including pure water, 0.1 M NaClO₄ aqueous electrolyte, toluene and dodecane. These authors observed both high and low sets of the conductance in all solvents. They also report that the conductance values are rather independent on the nature of the solvents within experimental uncertainties. They concluded that tunneling via solvent molecules does not contribute significantly to the measured conductance of alkanedithiols. However, the situation is rather different for dipolar and redox-active molecules, as many publications report,^{64,65} which show dependence of the conductance of redox-active molecules on solvent. Some theoretic studies focused on it,⁶⁵ and attributed such effect to the binding of solvent molecules to undercoordinated Au sites around the junction, since the affinity of the solvent molecules to Au binding sites and also due the induced dipole.
- **Effect of Temperature:** Selzer et al.⁶⁶ reported the first experimental demonstration of thermal effects on electron transport at the single-molecule level, they showed that inelastic processes and accompanied heat dissipation in a molecular junction can strongly influence the charge transport through molecular junctions. In Molecular Electronics, the effect of temperature is a very common technique used to determine the transport mechanisms, since they present different dependent conductances behaviors (see *Section “Transport Mechanisms in Molecular Junctions”, on Page 14*).

1.1.4 Techniques for the molecular conductance measurements

Many approaches and methods have been developed to obtain Molecular Electronic devices, we can divide them in two big families, according to the employed techniques, which are the based on *molecular array-based devices (MBD)* also known as ensemble junctions or monolayers, and the based in single-molecular junctions called *Break-Junction Techniques (BJ-Techniques)*.

In typical Molecular Electronics experiments employing the techniques based on *MBD*,^{67–69} is established an electrical circuit between two macroscopic solid electrodes, contacting them physically, with the particularity that at least one of both is coated with a molecular monolayer allowing the electrical measurement of electrode–molecules–electrode junctions. The obtained devices can be defined as mesoscopic, because electronically connects two bulky metal leads, but through a molecular/nano-junction, which dominates the transport of the circuit. Despite of it, is important to highlight that through this technique the conduction is effectuated via a physical contact where contribute all the molecules, thus any measured current feature is consequence of the collective effects due the molecular dense packing. On the other hand *BJ-Techniques* allows to contact single-molecules between two electrodes, since they are precisely separated with a defined gap which can be fitted by the target molecule. This apparent technical difficulty may be overcome by bringing two electrodes together or separating them apart mechanically. Thanks to using a *Piezoelectric transducers (PZT)* and mechanical actuation mechanisms as is explained in *Section “Break-Junction Techniques”* (Page 25), the gap can be controlled with subangstrom precision, making it possible to fabricate molecular junctions and measure the conductance.

The differences between both families are important to be discussed. Conceptually, a single molecule is a zero-dimensional (0D) object with dimensions smaller than the electron wavelength, while a monolayer has two dimensions (2D). Nevertheless, in both configurations the separation between the electrodes is normally less than ca 5 nm, i.e. charge transport occurs across a 0D. Nevertheless in *MBD* techniques the electron transport can be considered as a superposition of numerous, parallel single-molecule events.⁷⁰ Although remains unresolved how far the electron wave function is laterally constrained into a single molecule when these are close packed within a monolayer and if any generalization is possible. If such collective effect is understood, it can provide insights into the emergence of macroscopic charge transport, since molecules can interact with their surroundings. Therefore in the future, maybe *MBD* techniques offer a controlled way to manipulate and tune such contributions. In fact, is known that lateral coupling of energy levels also can facilitate the electron transport.⁷¹

Leaving aside any future application, at the present day, the essential research focused on the fundamental study of Molecular Electronics, is based on deepen the electronic effects due a molecular origin avoiding any cooperative effect, thus the *BJ-Techniques* represent the best tool since they allow the single-molecule trapping.

1.1.4.1 Molecular Electronics on Monolayers

The following points summarizes representative examples^{19,67–69,72–75} of state-of-the-art of the common methods used by Molecular Electronics based on *MBD* techniques All of them are based on the same starting idea. Mainly, a molecular film is sandwiched between two electrodes, such molecules are typically first immobilized on one electrode surface, via Self-assembled Monolayers (SAMs) or Langmuir-Blodgett methods. A second electrode is then placed on top of the molecular film. The contacting of the top electrode is usually the most difficult part of the measurement, and many methods have been developed. Aiming to prevent short-circuits between the electrodes, one must ensure that energetic metal atoms do not damage the molecular film and the deposited metal does not penetrate into the molecular film via defect sites to reach the bottom electrode, these details will be commented in each specific method.

1. **Hanging Hg drop junction** (Figure 1.9a): Is based on the mechanical attachment of a Hg drop to a surface of a SAM-functionalized electrode, obtaining low-resistive contacts (with solid metals or another Hg drop). Hg represents a valuable electrode material since is available in very high purity, is defect-free and as a metal behaves as perfect conductor. Although the explained method is efficient and cheap, Hg toxicity limits the method utility and applicability Also its affinity towards Au represents an important drawback because amalgams are formed very easily, causing short-circuits if Au electrodes are employed.
2. **Cross-wire junction** (Figure 1.9b): Two metallic wires of micrometric diameter behaving as electrodes, are contacted in a cross-like geometry (as show Figure 1.9b). One of the electrodes is covered with a SAM and positioned perpendicular the other, then both electrodes are brought gently into contact and the current measurements can be performed by applying a voltage difference between them. This approach also allows the incorporation of a magnetic field to combine with the conductance measurements.
3. **Nanopores** (Figure 1.9c): Name received by the fabrication of devices with nanoscale pores in a thin solid insulating membrane usually made of Si₃N₄ or SiO₂.^{76,77} The experimental configuration is characterized by a molecular monolayer inside the nanopore, which is sandwiched by two contacting metal layers. The nanopores (with a diameter of tens of nm) are commonly fabricated by lithography and plasma etching. Once the membrane is coated with a thin metal layer by one side, a monolayer is formed on the metal surface inside of nanopore followed by the fabrication of a suitable top contact.
4. **LOFO: Lift-off, float-on** (Figure 1.9d): Two-step method based on the following. (i) From a solid support is detached a metal film which then is floated on a sub-phase liquid (*lift-off*); later on the metal layer is (ii) attached

to the intended substrate (either SAM-modified or bare) in a liquid-mediated process (*float-on*).

5. **Nanotrasfer patterning** (Figure 1.9e): Is based on transferring SAMs from a poly(dimethylsiloxane) (PDMS) stamp onto a substrate, thanks to bringing a stamp with a thin evaporated metal layer in contact with a substrate, the metal layer is chemically bound to the substrate and released from the stamp, resulting in highly reproducible and well-defined structures with nanometric resolution even on large surfaces. This technique does not suffer from short-circuit during the device elaboration, being its main advantage, unlike what's happens with the direct evaporation of metals on SAMs.
6. **Nanoparticle array** (Figure 1.9f): Method based on the employment of Langmuir-Blodgett Monolayers of ordered 2D array of Au nanoparticles (Au NPs) encapsulated with the target molecules, once is formed, such monolayer is transferred by micro-contact printing with a PDMS stamp onto a suitable substrate. Thanks to this method can be measured simultaneously large amount of molecular junctions.

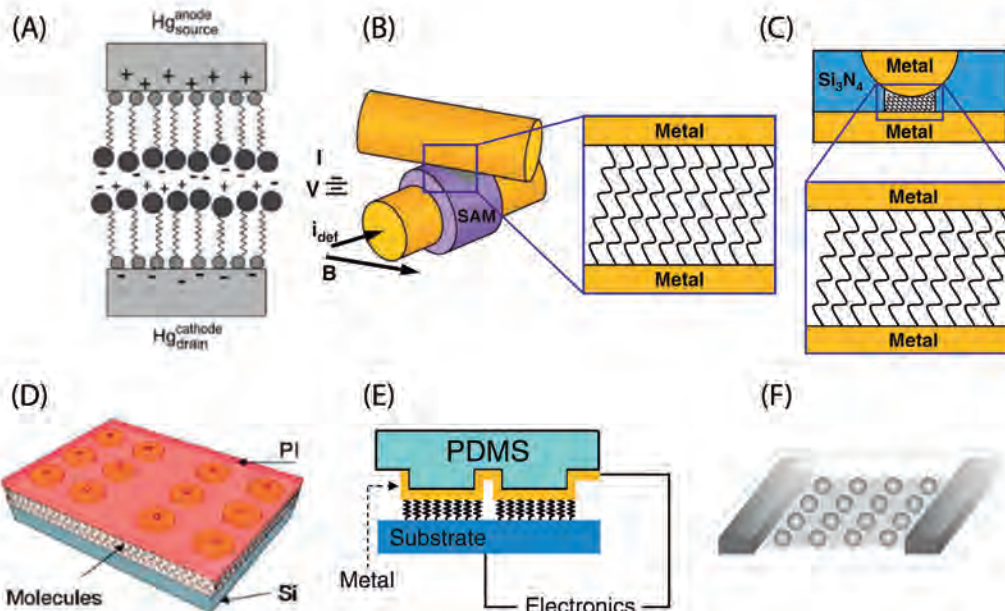


Figure 1.9: Schematic diagrams of different Molecular Electronics techniques based on Monolayers. Each panel corresponds to the described method in the text. Adapted from various references.^{68, 69, 72, 75}

1.1.4.2 Break-Junction Techniques

To achieve proper single-molecule current detection employing BJ-Techniques, are needed the following requirements *(i)* Provide a current signature to identify that the measured conductance is a result of not only the sample molecules, but also a individual single-molecule sample. This represents the fundamentals of any *BJ-Technique* and the main difference versus the *MBD* techniques. Also is important, to *(ii)* ensure that the molecule is properly attached to the two probing electrodes. This is achieved, as has been introduced previously, thanks the PZT since it not only provides controlled electrode separations with sub-angstrom precision, but also allows a robust stability which helps to the molecular attachment or trapping. Piezoelectricity represented the cornerstone to develop these techniques, because only thanks the application of such phenomena the PZTs actuators movement can be tuned precisely since their controlled mechanical stress (contractions and expansions) is ruled by means of an external applied high-voltage.

BJ-Techniques are extensively used and the three major types of BJ-Techniques described below are: *(i)* Mechanically controllable break junctions (MCBJ);⁷⁸ *(ii)* Scanning tunneling microscopy (STM) based break junctions (STM-BJ)⁷⁹ and *(iii)* Conductive probe atomic force microscopy based break junctions (CP-AFM-BJ).⁸⁰

Mechanically Controllable Break Junction Technique

The MCBJ technique was developed and introduced by Moreland and Ekin in 1985.⁸¹ They used a thin wire of a Nb-Sn filament mounted on a flexible glass beam. Using this *set-up* they measured electron tunneling characteristics of superconductors. But was in 1992 when Muller et al.,⁷⁸ coined the famous *Mechanically Controllable Break-Junction* name. An MCBJ device can be prepared manually by

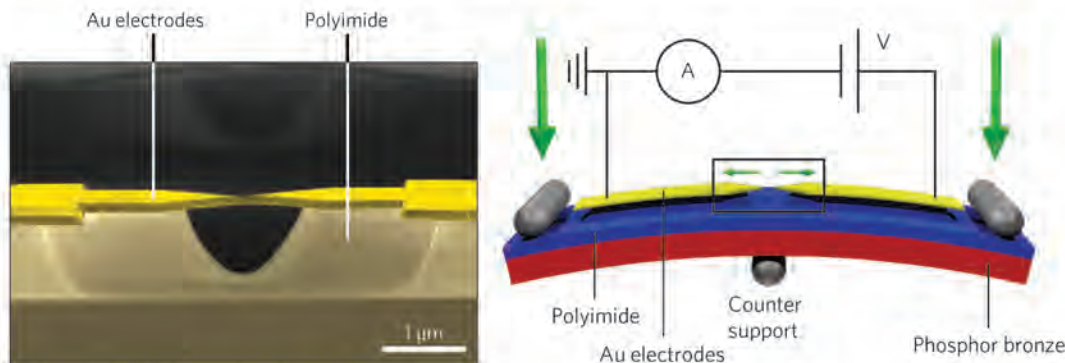


Figure 1.10: (Left) False-coloured SEM picture of a lithographically fabricated MCBJ device and (right) present layout for the MCBJ technique set-up. Adapted from Perrin et al.⁸²

fixing a metal wire, and in the middle of it, using epoxy glue and notching the central part of the wire to create a constriction point. The most recent way to create the nano-bridge (see Figure 1.10 left panel) is employing microfabrication techniques,

usually electron-beam lithography.⁸³ An accurate control of the nano-gap width, can be achieved since the bending is tuned by fixing the two ends of the substrate while pushing the middle part of the substrate vertically with the PZT displacement (see Figure 1.10 right panel), which is demagnified when the substrate is thin compared to its width. The system is also rather insensitive to external mechanical vibrations.

In the typical current measurements employing the MCBJ technique,^{78,82–87} first of all is dropped to the electrode pair, a droplet of an easily-evaporable solvent which contains the target molecules, aiming them to adsorb onto the electrodes. Since a flexible substrate is connected by two fixed beams on the top and one movable beam on bottom (see Figure 1.10 right panel), when the mechanical actuator, such as a PZT or a stepper motor, drives a pushing rod (movable beam) to bend the substrate, leads the elongation until finally breaks the metallic bridge on the substrate. After that, the caused nano-gap is then closed while maintaining a fixed voltage across the electrodes, during which time the current is recorded. Initially, the current grows exponentially, owing to electron tunneling across the gap. When the gap was decreased to a certain width, sometimes the current locked into a stable value weakly dependent on the gap width.⁸⁴ At that point, the first molecule is supposed attached to the opposite side, and any current signature can be associated to it.

STM Break-Junction Technique

STM-BJ technique was developed by Xu & Tao in 2003.⁷⁹ A similar *break-junction* approach of the STM was previously used to create metallic contacts for the study of conductance quantization of metal-metal contacts,⁸⁸ using such idea as a starting-point they designed a new technique which allows the *in-situ* creation of single-molecular junctions between a molecule and the STM tip and surface electrodes (see Figure 1.11 top). The description of this technique is elsewhere.^{36,79,89–91} Different reviews were used as guidance^{36,90} for the following detailed description.

The STM-BJ technique which quickly creates thousands of molecular junctions by repeatedly moving a STM tip into and out of contact with the substrate electrode in the presence of sample molecules in (*i*) the working solution surrounding the tip and the substrate electrodes or (*ii*) attached to them. The target molecules in the study have two anchoring groups which present affinity to both electrodes and can be trapped between them. Such process can be divided into three *stages* (see Figure 1.11 bottom): (*i*) The PZT drives the tip toward the substrate surface until it establishes contact. During such *contact* period, one or more molecules can bind to the tip electrode via the second (free) end group. (*ii*) The tip is *pulled* away from the substrate, and then the molecules break contact with one of the two electrodes individually, which is shown as a series of stepwise decreases in the current. (*iii*) The process is *cyclically repeated* until a large number of molecular junctions are created and measured. The conductance histogram of these molecular junctions exhibits peaks located near integer multiples of a fundamental value, which is used

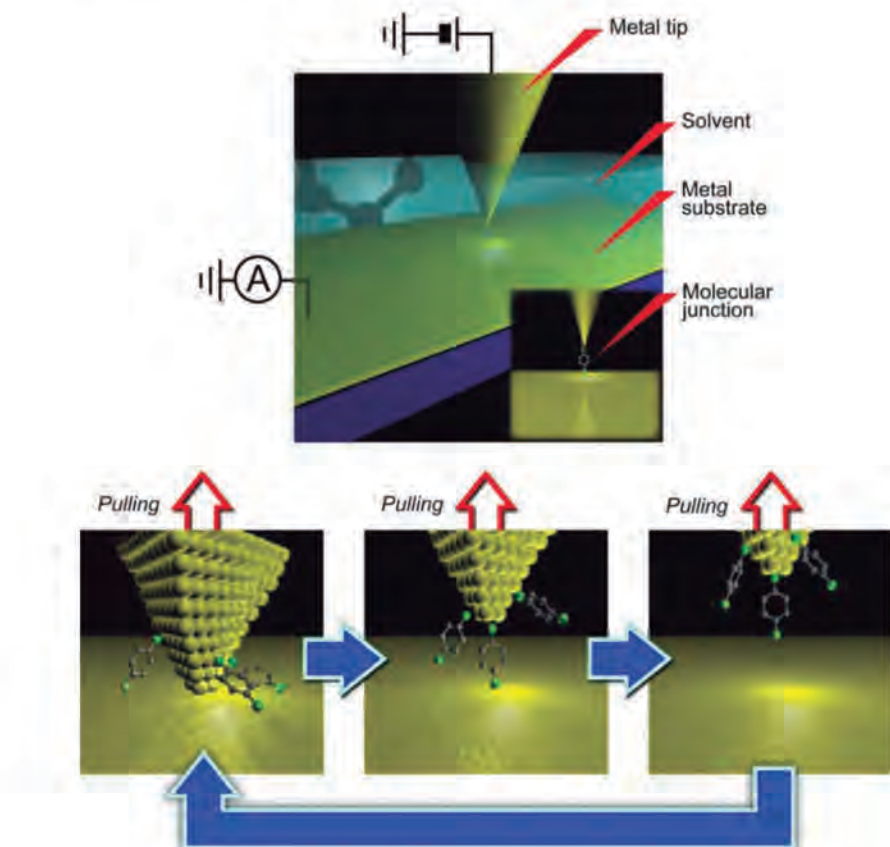


Figure 1.11: Schematic representation of the STM configuration (top) modified according to STM-BJ experiments. The molecular junction formation stages during the pulling described on the text are: (bottom-left) approaching, (bottom-center) formation of the molecular contacts and (bottom-right) breaking. Adapted from Tsutsui et al.⁹²

as a signature to identify the single-molecule conductance. During the approaching period, should be controlled the tip to either make contact with the substrate to form a Quantum Point Contacts (QPC) or prevent the formation of a point contact between the tip and the substrate.

Unlike most of the MCBJ experiments record the approaching processes, this technique focuses on the electrodes separation sequence (*pulling stage*). Because only those molecules bound between the two electrodes can be stretched until breakdown during the separation process, thus this technique measures selectively the conductance of those molecules bound to both electrodes. Is important highlight that as a consequence of the pulling of the tip, the number of molecules trapped between the electrodes during the *contact stage* is constantly decreasing, therefore the chances to detect just one molecule is very representative at the end of the *pulling stage*, just before the junction breakdown. Another difference is that the creation of the molecular junctions and the measurement of the conductance are performed in an organic sol-

vent or aqueous electrolyte, so one can easily introduce the sample molecules via the solution and control the electron transport through the molecules electrochemically. It is worth mentioning, that the STM-BJ technique since is based on a STM, can be used to imaging the substrate surface before performing the electron-transport measurement, so one can place the tip on an atomically flat area or move the tip laterally to a fresh area of the substrate during the measurement. This freedom comes at the cost of mechanical and thermal stability, however, which is typically not as good as the MCBJ.⁹³

Shortly after the STM-BJ birth, in 2004 Haiss and colleagues⁹⁴ proposed an alternative use of the STM, using the same STM-BJ's *set-up* but trapping the molecules spontaneously between the electrodes in a static motion-less way (see Figure 1.12 bottom). In this technique the electrodes are kept in a fixed distance adequate for the molecule dimensions and due the presented affinity of the molecule's anchoring groups for the electrodes they attach stochastically to them. To follow these contact events, the current is constantly monitored and every time that a molecule is trapped, the circuit is closed and the tunneling current through the gap is redirected through the molecule. As a consequence of these spontaneous contacts, current jumps are observed in the captured current, but since the molecular detachment is also spontaneous, is defined a telegraphic current output signal (see Figure 1.12 top).

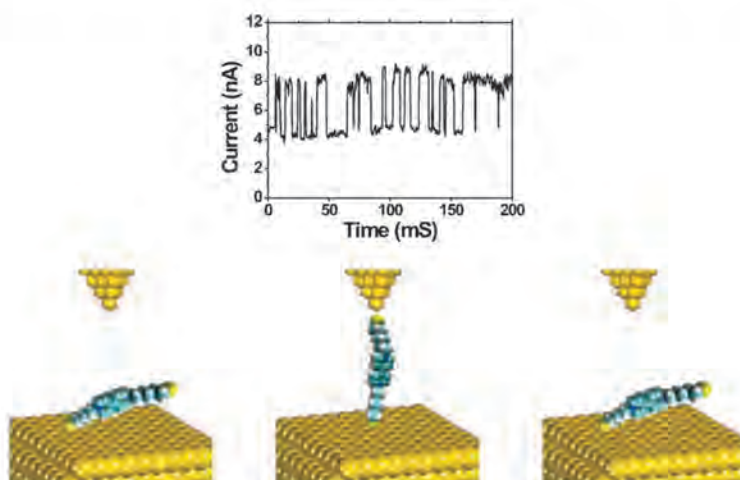


Figure 1.12: Schematic representation of the $I(t)$ technique. (Top) molecular junctions stochastically form and break in a constant height gap between STM tip and metal substrate. (Bottom) The junction formation and cleavage process is characterized by current jumps. Adapted from Nichols et al.⁹⁵

This thesis is based in the use of STM-BJ technique, and its both “uses” will be treated as different approaches of the same technique. The “dynamic” approach due the constant tip displacement will be called *tapping*, analogously to the AFM mode;⁹⁶ the “static” approach will be called *blinking* due the spontaneous and brief current jumps, as previous works proposed.^{43, 62, 97}

Conducting atomic-force-microscopy break junction

As a direct evolution of the STM-BJ technique, Xu et al.⁸⁰ employed the Atomic force Microscopy (AFM) in a similar way and clearly inspired by the STM-BJ technique⁷⁹ (as shows 1.13 left panel), explained above. For the first time, were measured the electromechanical properties of a single-molecules covalently attached to two Au electrodes by simultaneously recording the conductance and the force during the stretching of the junction using the conducting probe atomic force microscopy (CP-AFM). Such experimental approach allows the monitoring of two different signals: the breaking forces of the metal-molecule contacts and the molecular conductance, both simultaneously recorded during the stretching process. It is also applicable to a wide range of reactivity and recognition studies in solution and employing electrolytes even under electrochemical conditions. However, this field is currently still rather little explored.

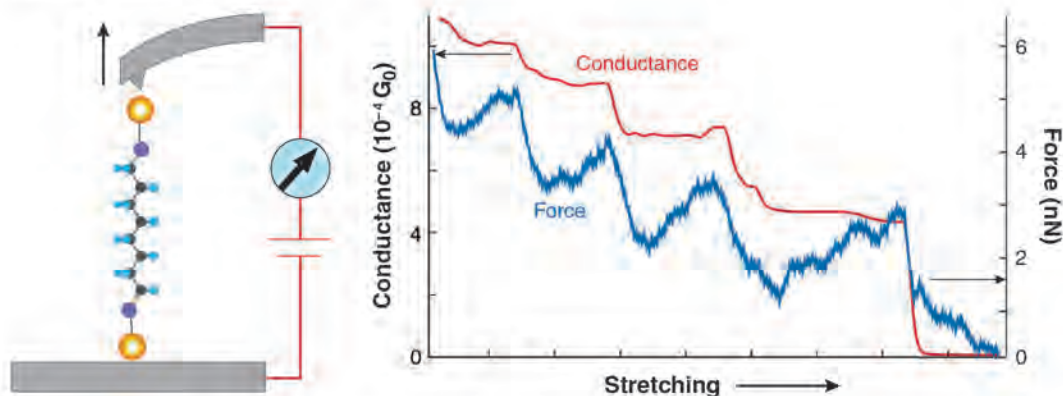


Figure 1.13: (Left) AFM modified according to CA-AFM-BJ technique. (Right) Simultaneous force and conductance captures of a molecular junction during the molecular breakdown. Adapted from Xu et al.⁸⁰

Figure 1.13 right panel shows and example of a simultaneous force and conductance measurements of a molecular junction during breakdown, each abrupt conductance decrease is accompanied by an abrupt decrease in the force, corresponding to the breakdown of a molecule from contacting the electrodes. Further pulling causes only a slight change in the conductance but an approximately linear increase in the force. When the force reaches a certain threshold, another molecule junction breaks-down, resulting in additional abrupt decreases in the conductance and the force. The conducting AFM break junction method also allows one to study the electromechanical properties of single molecules.

1.2 The tool: Scanning Tunneling Microscope

The STM is the basic and fundamental tool of this thesis. Ironically, it will not be used according the propose for it was designed for, because as was mentioned in the previous section, this microscope will be employed to trap molecules between its two electrodes, via the *tapping* and the *blinking* approaches. Nevertheless, is fundamental explain some basic notions of this microscope. However, the tunneling effect along its tunneling theory behind the STM, despite it involves quite interesting discussions, is not the aim of this thesis and can be found elsewhere.^{98,99} Thus the aim of this section is briefly explain how the STM works.

1.2.1 The Microscope

For a very long time in history, humans were limited to examine their environment with their eyes only. Things not visible to the naked eye simply remained inexplorable. This changed drastically with the invention of optical microscopes, opening up whole new worlds to investigate a new “dimension”, allowing to solve several scientific concerns (and of course, creating new ones). Unfortunately, the resolution of conventional light microscopy is limited to ca. 250 nm, due the diffraction of light.¹⁰⁰ Thus, a new technical limitation set aside, the impossibility to reach resolutions below 200 nm with conventional optical microscopes, leaving out another fascinating world: the molecular or atomic dimension.

Such situation changed with the creation of the scanning tunneling microscope (STM) by Binnig and Rohrer in 1981.²⁰ The development of this new technique by Binnig and colleagues^{20,101} has provided the scientific community an atomically resolved microscopic view of surfaces which previously could not be obtained by other techniques or at most only in a very indirect way. The experimental technique which has been described in several publications^{102–105} is conceptually simple (a scheme of a typical STM setup is shown in Figure 1.14 left panel): a sharp metallic probe or tip (see Figure 1.14 right panel), is attached to a *piezodrive*, which consists of three mutually perpendicular PZTs for the different spatial directions: x-PZT, y-PZT, and z-PZT. Since the application of a high-voltage, each PZT expands or contracts, through the applying of a sawtooth voltage on the x-PZT and a voltage ramp on the y-PZT, the tip scans on the xy plane. Using the coarse positioner and the z-PZT, the tip is brought into close proximity (fraction of a nanometer) of a sample surface (conductive or semiconductive), therefore the electron wavefunctions in the tip overlap electron wavefunctions in the sample surface. A finite *tunneling conductance* is generated. By applying a bias voltage (V) between the tip and the sample, a *tunneling current* I_T is generated and captured to map the sample surface through an atomic level thanks to moving (*scanning*) the tip by the high precision of the *piezodrive*. The distance between the electrodes allows the reconstruction of the scanned surface from its magnitude, since the exponential relationship¹⁰⁶ between I_T and distance since the Schrödinger equation imposes that the wavefunction cannot go to zero abruptly (the wavefunction and its derivative must be continuous and

derivable at all points), thus according to the theory^{98,99} the probability of finding the electron ($|\psi|^2$) follows an exponential decay with the distance. This is the fundamental expression for Electron Tunneling and it was attested experimentally in the study semiconductors.¹⁰⁷⁻¹⁰⁹

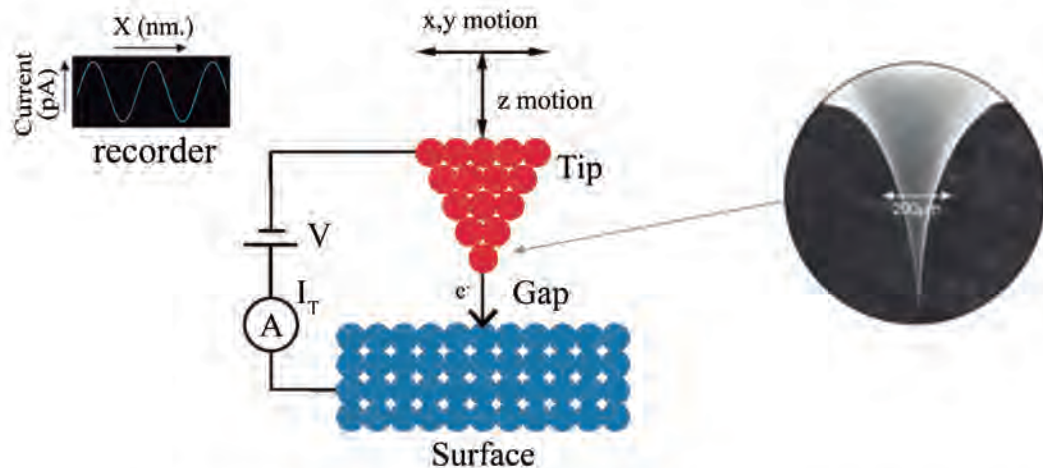


Figure 1.14: (Left) Schematic diagram of the STM technique. The scan consists of a constant monitoring of the tunneling current (I_T) at different positions thanks to the tip motion controlled by x, y and z - directions. With the captured current lines, a map of the surface is computationally produced. Adapted from Bowker et al.¹¹⁰ (Right) Detail of STM sharpened tip (SEM picture). Adapted from Cuevas.²¹

The most commonly used convention of the polarity of V is that the tip is *virtually grounded*, thus V is the sample voltage. If $V > 0$, the electrons are injected from the occupied states of the tip into the empty states of the sample. Contrary, If $V < 0$, the electrons are injected from the occupied states of the sample into the unoccupied state of the tip. Employing a current amplifier, I_T is converted to a voltage by the current amplifier and processed in distinct ways depending the employed modes (constant current or height), explained at below.

1.2.2 Working principles

Originally, the STM was mainly used for investigating the surface topography, but nowadays is common to probe the local density of states (LDOS) of a sample surface with extremely high spatial resolution, representing an exceptional approach for the STM. The STM can work in two different modes for imaging: The constant current mode and the constant height mode, explained below:^{101,103,105,106}

- The *constant current mode* (see Figure 1.15 left panel) uses a bias voltage between electrodes and a well defined *set-point* (I_{SP}), which is kept as a constant current value thanks a feedback system. The computed difference between I_T and I_{SP} is amplified to drive the z-PZT. The phase of the amplifier is employed to provide a negative feedback. If due to the topography of the sample

or a change in the LDOS the I_T suddenly increases or decreases from the I_{SP} value, via the high precision *piezodrive*, the tip is retracted from the surface or brought closer to it, respectively. Thus, an equilibrium for the z-position is established. As the tip scans over the xy-plane, a 2D array of equilibrium z-positions of the tip is recorded, translated to height and stored in the computer memory. STM is not sensitive to the topography only but also to the LDOS. STM measures actually the *iso-surfaces* of the LDOS near the ϵ_F where all electronic states in the energy interval $[\epsilon_F; \epsilon_F + eV_{Bias}]$ contribute to the I_T . Obviously, the LDOS is affected by the sample topography, but especially for flat surfaces on atomic length scales, where the effects are more significant and thus, the technique mainly is not dependent on the topography. The constant current mode represents the most used approach for the STM technique.

- The *constant height mode* (see Figure 1.15 right panel) also uses a V_{Bias} between the microscope electrodes but the surface is scanned at a constant height without any feedback loop while the change in I_T is recorded. Since the samples are rarely completely flat is necessary an electronic correction of the local sample slope. At every image x,y-point the variation of the I_T is recorded and used for the reconstruction of the sample surface. In contrast to the prior mode, the image is not taken via the *iso-surface* of the LDOS, but at varying LDOS at the same tip-sample distance. Since no feedback is used, in this mode can be acquired faster. But the main drawback is that can only be employed to rather smooth surfaces, therefore its use is not very extended, and is reduced to achieve extremely high-resolution maps of extremely flat surfaces with atomic or molecular features.

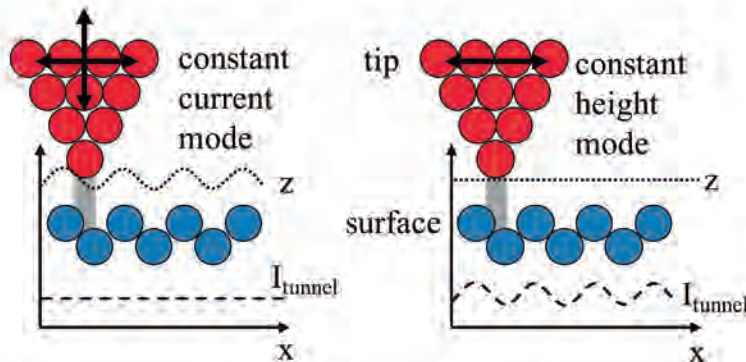


Figure 1.15: Atomic representation of a signal from STM under the (left) constant current mode and (right) the constant height mode. Adapted from Leach et al.¹⁰⁵

For both modes, the topography or the plotting of the LDOS of the surface is processed and displayed on a computer screen, typically as a monochromatic-scale image, where the bright spots represent high z values (protrusions), and the dark spots represent low z values (depressions).

1.3 The concept: *External fields and molecules*

As we have seen, constant evolution of electronics moved it on to the molecular scale, becoming Molecular Electronics. Future basic functionalities based on this miniaturized evolution of the electronics, analogously to its predecessors (classical electronics and microelectronics), also should be based on 0/OFF and 1/ON states, which have to be associated to two opposite high and low conductance stages of reversible molecular systems.^{36, 89, 90}

Usually, such reversible behavior is ascribed to switchable conformational modifications of the molecules, typically conducted through chemical reactions.^{9, 47, 111} They present different important drawbacks such as a switching behaviors not fully-reversible, conversion cycles quickly degraded and low switching efficiency rates; as well as the technical difficulties to control the switching behavior of the system using chemical species a part from the reactants as well as their possible inherent contamination and side reactions, which can affect to the efficiency. Replace these chemical species by external stimuli, represents the best option to tuning the employed molecules in an efficient way, preventing from the reactivity drawbacks.

Light was proposed as a strong candidate as reported many previous works of single-molecule conductance based on photochemistry.^{112–115} This kind of molecules, called photo-switches, do not contribute in a significant way for the field since they are chemically difficult to obtain, thus the molecule's diversity and availability is really low. A part of the mentioned inconveniences also they present another inherent drawback as their chemical instability and the consequent strict conditions to operate with them, hampering even more the real applicability of their based-technology. In summary, employing light as a stimulus does not represent the best solution to improve Molecular Electronics field.

To advance in the robustness and real applicability of Molecular Electronics, the explained drawbacks require to be solved, as well as is needed to find stimuli which offers an exhaustive control of the molecular changes, durability, lacks on contamination and degradation as well as ensure high efficiency on a broad range of molecules. The proposed alternatives in this thesis are the magnetic and the electric force fields, because they have the prospective to overcome many of the drawbacks as well as offer some of the required capabilities.

The magnetic field in a strict way does not cause noteworthy structural changes to molecules, because mainly affects to the electronic structure, but as we are talking about Molecular Electronics, it represents a very strong candidate since the electric current can be significantly affected by a magnetic field. The modulation of the resistance of a system depending on applied **External Magnetic Field (EMF)** is called magnetoresistance (MR), and represents the basis of the Spintronics field. The proposal of the first part of this thesis is based on the use of such EMF as a tool to tune single-molecule conductance externally preventing from any kind of reactivity and the associated explained problems.

On the other hand, the **External Electric Fields (EEF)**, can be used as an alternative to conventional chemistry, aimed to tune the molecular interactions between reactants (chemical reactions) in an efficient way in addition to avoiding the use of additional chemical species and the involved drawbacks. The main advantages of these force fields are tunable orientation, specificity and ease offered due its external control as is explained detailed in the following *Section “Electric fields and molecules”* (Page 50). For this reason, the second part of this thesis will be based on the use of EEFs, modifying precisely the orientation and strength with the aim to control *in-situ* the specific interaction between two molecules and create efficiently molecular junction. Representing also, an alternative novel use for Molecular Electronics and specially the Break-Junctions Techniques as platforms to detect and manipulate molecular interactions.

1.3.1 Spintronics: When electronics and spins meet

The concept Spintronics as the word suggests, is the mixture between two concepts, electronics and spin. In a narrow sense Spintronics refers to spin-electronics, the exploitation of both electron’s degrees of freedom the charge and spin electrons, usually studied through charge phenomena of spin-polarized transport.^{116–122} The goal of applied Spintronics is to find effective ways to control the current or the accumulated charge through a EMF, as well as the inverse role controlling the current by electric currents or gate voltages and its associated effects over magnetic properties. Therefore, the fundamental studies of this emergent field are based on characterizing electrical and magnetic properties of the objective systems via the presence of equilibrium and non-equilibrium spin populations, as well as spin dynamics.^{116, 120, 121} Such spin phenomena are usually studied combining metals, semi-metals and semiconductors in sandwiched hetero-structures. Despite this emerging field is very recent, the amount of fundamental and applied research is striking broad and difficult to summarize, but many author such as Zutic,^{118, 122} Hirohata,¹²³ Fusil¹²⁴ and Sanvito¹²¹ did this challenging task of summarize few more than one decade of work in their extended reviews, which served largely as guide for the short summary for this Section.

Spintronics is one of the emerging research fields with the ultimate goal to obtain practical device schemes that would enhance functionalities of the current charge based electronics microelectronics as well as nanoelectronics and has been growing very rapidly started after the discovery of Giant Magnetoresistance effect in (GMR) 1988 by Baibich and colleagues,¹²⁵ but the first commercial product using GMR was available many years after, in 1994 and was a magnetic field sensor which nowadays already has been used practically in all the produced hard disk drive (HDD) heads until the apparition of solid state devices (SSD).

As is mentioned above, the breakthrough in this field was the discovery of GMR observed in metallic multi-layers via spin-dependent electron transport.^{125, 126} Such phenomena happen when directions of the magnetic moments are manipulated by

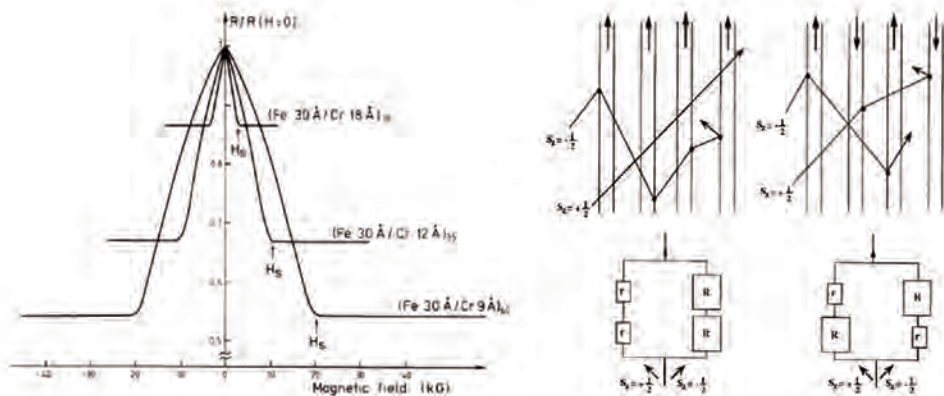


Figure 1.16: GMR signals (left) with schematic model's explanation of the two-current model (right). Adapted from Hirohata et al.¹²³

EMFs that are applied to the materials (see Figure 1.16 left panel) made from layers with different alignment (see Figure 1.16 right panel). If the ferromagnetic layers are antialigned (opposite spin alignment), the spin-dependent scattering of the carriers is maximized, and the material shows a high resistance. Oppositely, when the magnetic moments of ferromagnetic layers are parallel oriented,^{125, 127} the spin-dependent scattering of the carriers is minimized, causing the lowest resistance scenario for the material. The disposition of the layers and the current flowing between them defines the two possible structural geometries, the current-in-plane (CIP) (Figure 1.17 left panel) and current-perpendicular-to-plane (CPP) (Figure 1.17 right panel) geometries. GMR effect is present for both cases, and its amplitude and sign are determined by the spin-dependent scattering “times” in the different layers and at their interfaces.¹²⁸ Nevertheless, for GMR applications the CIP geometry is mostly used, and contrary the CPP geometry, first realized by Pratt and colleagues,¹²⁹ is easier to analyze theoretically.¹³⁰

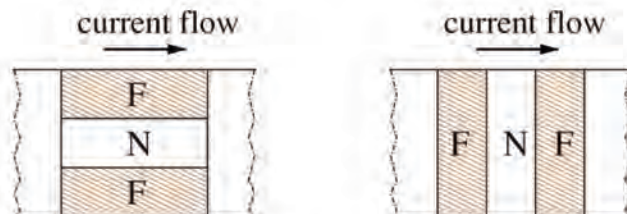


Figure 1.17: (Left) Schematic illustration of the current in plane (CIP) and (right) the current perpendicular to the plane (CPP) giant magnetoresistance geometry. Adapted from Žutić et al.¹¹⁸

But, how is designed a spintronic device? Three key-stage are required: *injection* of a spin-carrier, *manipulation* and *detection*. The way to combine them is the following, first has to be generated a spin population in non-equilibrium within a given material (*injection stage*), i.e. spins must be prepared in the desired initial configuration. After it an external stimulus should be applied to orient/polarize in a

predefined direction the initial spin population in a controllable way (*manipulation stage*) and finally the result of the manipulation should be detected (*detection stage*). Each mentioned stage is explained in detail below:

1. The Spin-polarized injection exists in magnetic materials and non-magnetic materials:

(a) Spin-polarized injection can occur naturally when a junction is made by a magnetic metal or metallic alloys for which there is an imbalance of the spin populations at ε_F (see Figure 1.18 left panel). This imbalance commonly occurs in ferromagnetic metals because the available density of states (DOS) to spin-down and spin-up electrons is often nearly identical, but their states are shifted in energy with respect to each other (see Figure 1.18 right panel). This shift results in an inequivalent filling of the bands, which is the source of the net magnetic moment for the materials, but it can also cause the spin-carriers transport at the ε_F to be unequal in polarization, number and mobility. Such asymmetry causes a net spin-polarization in current measurement, but the sign and magnitude of that spin-polarization depends on the specific experimental conditions such as the employed materials, thus the nature of the specific spin-polarized carriers and the electronic energy states associated with each material must be identified in each experiment.^{116,119}

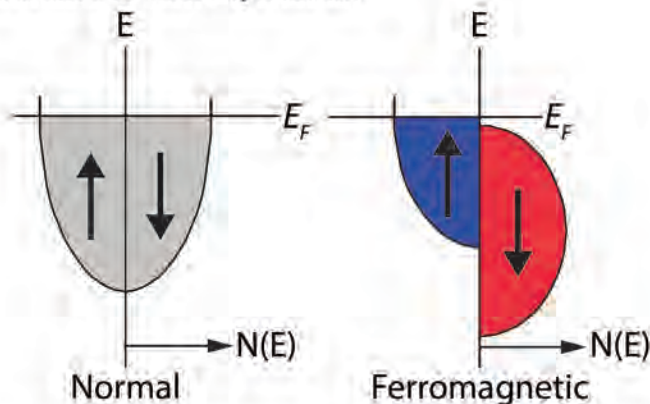


Figure 1.18: Schematic DOS of a non-magnetic “normal” metal or alloy with balanced spin populations (left) and for a ferromagnetic metal or alloy with unbalanced spin populations (right).

- (b) Spin-polarized electrons also can be generated in non-magnetic materials via using the following methods: spin injection from an interfaced ferromagnet, EEF, circularly polarized photoexcitation, thermal gradients or Zeeman splitting. Or use half-metallic ferromagnets (HMF) and dilute magnetic semiconductors (DMS), attached to a non-magnetic metal or semiconductor through an ohmic contact behaving as tunnel barrier. External fields are used because cause spin-polarized carriers motion in a favorable direction, such as the spin Hall effect (under electric fields) or

circularly polarized light, which excites spin-polarized electrons in a semiconductor. The reverse effect generates circularly polarized light emission by a spin-polarized electron current. This can be extended further to spin generation by electromagnetic waves, including spin pumping and high-frequencies spin induction. In addition, a thermal gradient has been found to produce a spin-polarized carrier flow due to a spin Seebeck effect.¹¹⁶ In a DMS, Zeeman splitting induces spin imbalance at the ε_F .¹¹⁶

Despite several methods are known to inject Spin-polarized populations, the associated injection mechanisms between interfaces and layers or molecules is still unclear and the factor that governs such processes remain subject of discussion.^{120, 131, 132}

2. Spin manipulation can be carried out employing different external stimuli like magnetic^{117, 124} or electric fields,^{117, 123, 124} light (optical pumping or orientation),^{117, 118} temperature¹¹⁸ or even mechanical force¹²⁴ to predefine a polarized direction of the injected electron population.
3. The detection stage typically relies on sensing the changes in a captured signal caused by the presence of nonequilibrium spin in the system. Usually the common aim in spintronic devices is to maximize the spin detection sensitivity to the point that it detects not the spin itself, but changes in the spin state and is achieved using analogous techniques depending on such changes. Exists several options. The simplest one is based on current detection,^{117, 118} but also can be find potentiometric techniques¹¹⁷ and several based on magnetometry^{123, 124} (X-ray resonant magnetic scattering, NMR or SQUID) or spectroscopy (circularly polarized light detection¹²³ and circular polarization of the electroluminescence¹¹⁷).

The described three stages are combined in several different ways to obtain a spintronic device, the most illustrative and basic thus extended, is the spin-valve system explained on the next Section, which constitutes the basis for Spintronics mechanisms and phenomenology.

1.3.1.1 Spin-valves

The prototypical electric spin-device is the spin-valve (see Figure 1.19 top), which consists of three essential ingredients: two magnetic metal leads (normally made by transition metals) and a third isolating non-magnetic, sandwiched between them. In such sandwiched triple structure the resistance depends on the relative alignment of the electrodes' magnetization (parallel or antiparallel), as dictates the GMR. A non-equilibrium spin population (see Figure 1.19 bottom) current is injected from the injector to the non-magnetic material. When it reaches the current detector the resistance of the device will depend on the spin-polarized direction of the injector and the detector leads.

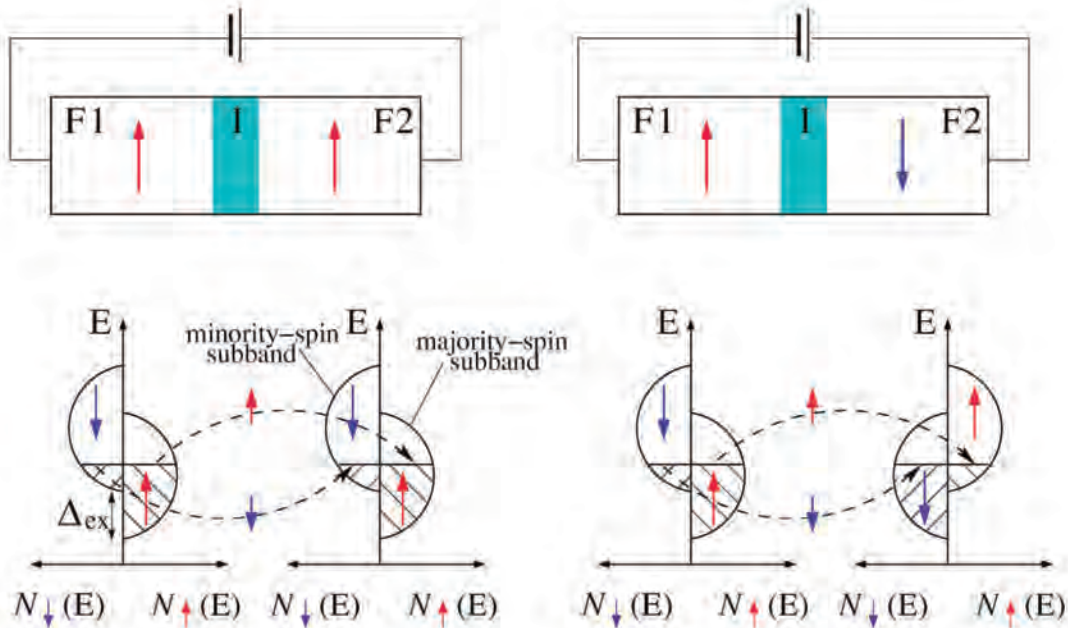


Figure 1.19: Schematic illustration of electron tunneling in ferromagnet/insulator/ferromagnet tunnel junctions: parallel (left) and antiparallel (right) orientation of magnetizations with the corresponding spin-resolved DOS. Arrows in the two ferromagnetic regions represent the bands with the majority spin-orientated population. Dashed lines depict spin-conserved tunneling. Adapted from Zutic et al.¹³⁸

This occurs as a consequence of the individual resistances of the two-polarized spin-channels. In general the relative conductance of the two spin-channels of a magnetic material is defined by its spin-polarization, P_n (see Expression 1.20). This is a property related to the electronic structure of the material itself and also to the experimental technique used to measure it, can be understood by the following expression:

$$P_n = \frac{N_{\uparrow}\nu_{\uparrow}^n - N_{\downarrow}\nu_{\downarrow}^n}{N_{\uparrow}\nu_{\uparrow}^n + N_{\downarrow}\nu_{\downarrow}^n}, \quad (1.20)$$

where N_{σ} is the material's DOS at the ε_F for spin σ ($\sigma=\uparrow$ for majority electrons and $\sigma=\downarrow$ for minority) and ν_{σ} is the spin-dependent Fermi velocity. The Fermi velocity is weighted differently depending on the particular experiment, with $n=0$ for photoemission measurements and for tunneling across amorphous barriers, $n=1$ for ballistic transport and $n=2$ for diffusive conduction. Note that, as a consequence of the definition of P_n , the same material may have a substantially different polarization depending on the specific experiment carried out or on the specific length-scale examined.¹³³ The place where spins are injected is different from the one where they are detected, analogous to an electric circuit, therefore the electrons spins must be driven across the non-magnetic material. In such transfer processes, they will continuously attempt to reach their equilibrium state by interacting with

the environment. At such equilibrium in a non-magnetic material there is no spin imbalance so that during its motion the electron lose its initial spin-polarization. Two magnitudes characterize the spins' interaction effects with their surrounding: the spin-relaxation time, τ_S , and the spin-relaxation length, l_S . The spin-relaxation time is the average time that the electron spin takes before changing its original direction. In order to help the understanding, a clear analogy with nuclear magnetic resonance, can be performed with such mechanism because one can define the longitudinal, T_1 , and the transverse, T_2 , spin-relaxation times. However, in a spin-valve experiment there is no direct access to these two quantities separately, since the injected electrons do not have a defined phase relation (they are not coherent). Hence the more general definition of τ_S must be used. Instead the average distance travelled by a spin defines the spin-relaxation length. Clearly τ_S and l_S are simply related by $l_S = \mu \tau_S$, where μ is the average electron velocity. The magnitude of l_S relatively to the spin-valve nonmagnetic spacer thickness, L , determines the ability of the spin-valve to work. In fact, if $l_S < L$, the spin-polarization of the injected current will be completely lost by the time the electrons reach the detector. As such the resistance of the entire device does not depend on the direction of the magnetization vectors of the electrodes. In contrast if $l_S > L$ some spin-polarization will survive the motion in the non-magnetic spacer and the total resistance will depend on the spin-valve magnetic state. This simple concept however suffers of another obstacle, present even if $l_S = \infty$. This is known as the resistance mismatch problem. The equivalent resistance of a spin-valve is obtained by adding in series the resistances of the electrodes (spin dependent) and that of the spacer (spin independent). As such, if the resistance of the spacer is much larger than that of the electrodes, the total resistance of the device will be only weakly spin dependent.

1.3.1.2 Tunneling Magnetoresistance

Going deeper the nanoscale, exists the tunneling magnetoresistance (TMR) effect, is a GMR effect presented by a metallic tunneling junction (MTJ) in CPP configuration (see Figure 1.20 left panel). So first of all should be explained what is a MTJ. Mainly, is heterostructure formed by two electrodes separated by a ultra-thin dielectric layer (tunnel barrier) of a thickness ranging from a angstroms to a few nanometers, where the electrons can travel from one electrode to the other by tunneling through the tunnel barrier resulting in electrical conduction. Since that such junctions are tri-layered structures, they are constituted originally mimicking the spin-valves devices using thin non-magnetic spacers (behaving as the tunnel barrier) sandwiched between two ferromagnetic electrodes. As a consequence, the polarized electrons can travel across the barrier when are injected from one electrode to the other, polarized parallel or antiparallel relative magnetization orientations between them, thus determining to the resistance of the system (see Figure 1.20 right panel).

The efficiency of TMR depends on two parameters, (*i*) the spin-polarization of the DOS at the interfaces formed by the tunnel barrier and the electrodes as well as (*ii*) the decay rates of the tunneling wave functions in the barrier.

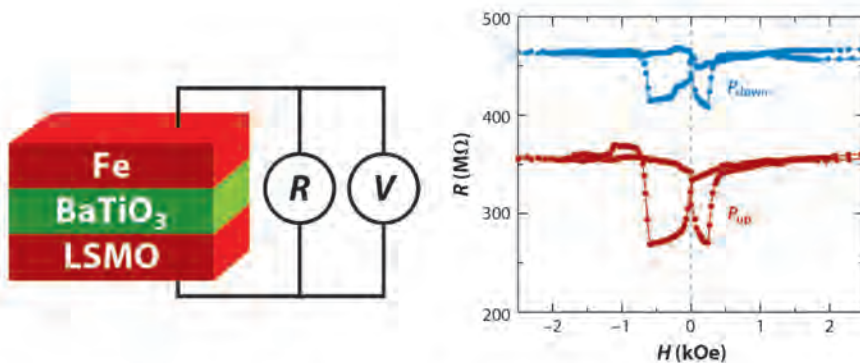


Figure 1.20: Example of spintronic device based on TMR effect (left). The amplitude of its TMR response (right) depends on the direction of the ferroelectric polarization in the Ba-TiO₃ barrier, reflecting electrical control of the spin-polarization of the BaTiO₃/Fe interface. Adapted from Fusil et al.¹²⁴

Two schemes have been proposed to achieve magnetoelectric control of TMR.¹³⁴ One scheme relies on the control of the magnetic properties of one electrode off MTJs deposited onto a ferroelectric, piezoelectric, or multiferroic material.¹³⁵ The other scheme involves the use of ultrathin ferroelectric or multiferroic layers as the tunnel barrier.¹³⁶

1. In the first scheme, the device requires three electrical terminals, the two electrodes of the MTJs and the third terminal as the bottom electrode to apply a gate-voltage across the ferroelectric. This setup difficult the fabrication process, and so far, there have not been effective experimental advances.
2. In the second proposed scheme, contrary, only two terminals are needed to both pole the ferroelectric barrier and probe the junction magnetoresistance. Garcia et al.¹³⁶ reported, in LSMO/BaTiO₃/Fe junctions, nonvolatile control of the TMR amplitude by voltage¹³⁶ due to the interfacial dependence of the spin-polarization of Fe with BaTiO₃ on the ferroelectric magnetic polarization direction.^{137–139} Such device achieved more than 300% TMR rate. Another prominent work was reported by Pantel et al.¹⁴⁰ where an inversion in the sign of the TMR was induced by ferroelectric polarization switching, due the employed LSMO electrode¹⁴¹ lost its spin-polarization just below 300K and they worked at Low Temperature (LT) regimes.¹⁴² MTJs with relatively thick (1.5 nm) MgO layers,^{143,144} allows (under a static EMF) the tuning of the MR effect electrode by a voltage inducing reversible switching of the junction magnetic state between parallel to antiparallel at RT (Room Temperature) conditions.

Although the TMR ratio can theoretically be almost 50% with conventional FM metals, a high TMR ratio was not reported until 1995 by Miyazaki and Tezuka with Fe/Al₂O₃/Fe junctions.¹²³ The maximum TMR ratio has been reported with an

amorphous Al-O tunnel barrier in an MTJ with structure Si(001)/Si₃N₄/Ru/CoFeB/Al₂O₃/CoFeB/Ru/FeCo/CrMnPt.¹²³ In these MTJs, the interfaces between ferromagnets and insulators are not sharply defined and the insulators cannot be treated as an ideal barrier due to defects and grain boundaries. But without doubt the most extended TMR use is the implantation to the HDDs' read-heads, realized by Seagate in 2004,¹⁴⁵ and nowadays commonly used. Besides, ballistic transport was achieved in 2004 causing TMR ratios of over 1000% at RT due Fe(001)/MgO interface with oriented MgO barriers.^{146,147} Also coherent tunneling was achieved for TMR showing a ratio over 100% at RT,^{148,149} according it is expected to reduce the HDDs' read-heads size in an HDD as well as allowing the improvement of the read/write cycles in the MRAM memories (see Figure 1.21). Volatile memory also based on TMR but not significantly expanded in the common informatics market.

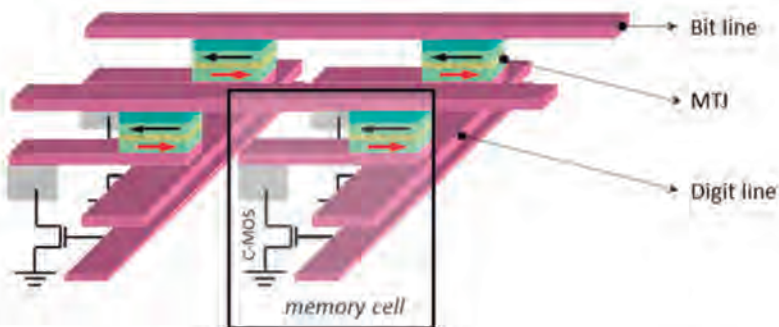


Figure 1.21: Architecture and the writing and reading scheme as well as the basic MTJ cell (inset) used in first-generation MRAMs. Adapted from Prejbeanu et al.¹⁵⁰

1.3.1.3 Magnetic fields and molecules: Molecular Spintronics

As we have seen in the previous Section, the general idea behind Spintronics is the study and manipulation of the spins' response to an external stimulus with the future aim to use it to develop "spintronic" memories, data storage or sensing nano-devices. Nanotechnology has been a valuable tool to advance in the Spintronics field's, in fact served to obtain very efficient spintronic-devices. Basically they are based in the detection of the MR effect through current measurements of heterojunctions,^{123,124,151} sandwiching different metals^{152–155} or metals with semi-metals^{156,157} as well as metal oxides¹⁵⁸ or even organics layer like buckyballs.¹⁵⁹ Unfortunately, the costs and the lack of the required efficiency of the mentioned spintronic-devices, forced to move the field to the next step: the use of single-molecules' The *Molecular Spintronics* field has born.

This new single-molecular dimensionality could represent the solution to obtain many desirable capabilities such as longer spin relaxation times¹⁶⁰ allowing a higher efficiency due less-power consumptions,¹⁶⁰ increased speed operation for computational devices¹⁶¹ and high Curie temperatures ideal for non-volatility memories;^{162,163} all of them along with low production costs and self-assembling capa-

bilities.¹²¹ As a consequence, Spintronics is now evolving to a second-generation emerged as a new and more complex field at the frontier between molecular engineering, surface science, physics, chemistry or biology. Such jump to the molecular dimension has born as a parallelism of the Molecular Electronics, a direct evolution also presented by (micro)electronics. Therefore, Molecular Spintronics is not starting experimentally from zero because can be considered a complement for such Molecular Electronics field, because is adding to it the spin degree of freedom. Molecular electronic existing tools offer a double contribution for Spintronics field, the basis to developing spintronic devices and the appropriate functional test-benches for fundamental studies of the field.¹²⁴

The first for Molecular Spintronics device was pioneering developed by Tsukagoshi and co-workers via multi-walled carbon nanotubes (MWNT) in 1999.¹⁶⁴ Such carbon-based device behaved as spin-valve devices since the MWNT acted as an effective spin channel for injected spin-polarized current.¹¹⁹ Later on, Dediu and colleagues in 2002 tune the resistance of a sexithienyl junction under the application of an external EMF by using polarized electrodes,¹⁶⁵ in fact, it represents the first MR evidence employing organic molecules. From these two revolutionary Molecular Spintronic devices, the research has now been widely expanded, and can be classified in two families regarding the junction's components and their magnetic capabilities as: (*i*) magnetic molecules on non-magnetic electrodes and (*ii*) non-magnetic molecules on magnetic electrodes.

1. The former case is based mainly on molecular junctions using “single-molecule magnets”(SMMs). SMM are metalorganic compounds (see Figure 1.22 left panel), specifically polynuclear metal complexes surrounded by bulky ligands (often organic carboxylate ligands) which exhibit intrinsic magnetic features such as magnetic moment, extremely high anisotropy and slow magnetization relaxation at LT, with highlighting records of anisotropy barriers of ca. 100 K and relaxation time of years below the 2K.¹⁶⁶ In addition, underneath their blocking temperature, at LT regimes of course, they present analogous behavior to the macroscopic magnets showing hysteresis curves (see Figure 1.22 right panel-top), being this behavior one of the reasons to use them massively to develop spintronic devices. Since their usual size between 1 and 10 nm, they also present some quantum phenomena, like the quantum tunneling of the magnetization^{167–170} (see Figure 1.22 right panel-bottom) or long coherence times.^{171–173} Thanks to all the mentioned capabilities, SMMs represent strong candidates to lead the progress on Molecular Spintronics field because they show great prospects as essential units for quantum information processing or for high density information storage applications.^{174–176}

Nevertheless, such capabilities are exclusively to the LT regimes and it represents a serious drawback, particularly the low blocking temperature since it characterizes their fundamental feature to base on the applied-technology development, e.g. the “drosophila” SMMs based on Mn₁₂, has a blocking temperature around 4 K¹⁶³ and TbPc₂ SMMs reach up to 40K,¹⁷⁷ being the

latter one of the highest achieved temperature case. Despite the great efforts to synthesize SMMs with blocking temperatures closer to RT, no significant advances were achieved, therefore nowadays it represents a significant drawback to develop any realistic application.

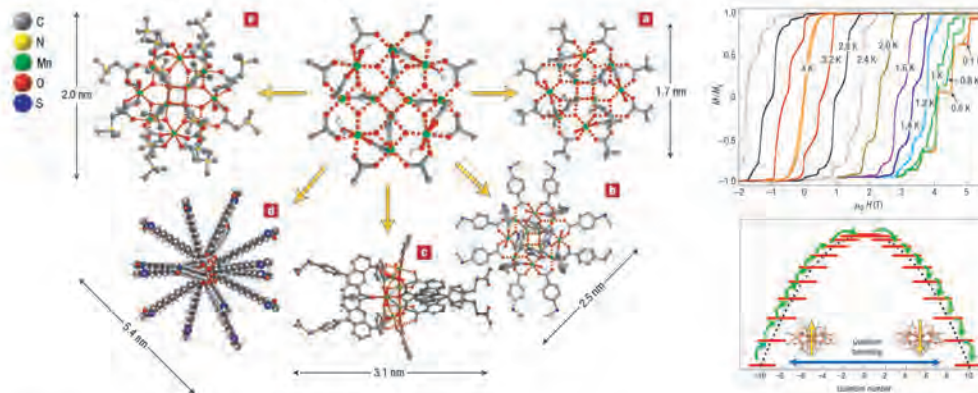


Figure 1.22: Overview of Mn_{12} complexes with different ligands for surface functionalization (left). The central figure shows a bare magnetic basic functional unit $Mn_{12}O_{12}(CH_3COO)_{16}(H_2O)_4$ with minimal ligands. (a-e) Show different ligands attached to Mn_{12} , highlighting the extreme functionalizability of molecules. All structures were determined by X-ray crystallography, except d, which is a model structure. Example of a hysteresis loops of a SMM at different T and a constant field sweep rate of $2 \text{ mT}\cdot\text{s}^{-1}$ (right-top). Diagram example of the energy landscape of a SMM with a spin ground state $S=10$ (right-bottom). The magnetization reversal can happen via quantum tunnelling between energy levels (blue arrow) when the energy levels in the two wells are in resonance. Phonon absorption (green arrows) can also excite the spin up to the top of the potential energy barrier with the quantum number $M=0$, and phonon emission descends the spin to the secondwell. Adapted from Bogani et al.¹⁶³

2. The non-magnetic molecules trapped between polarized electrodes, should gather certain properties essential for Molecular Electronics uses like low resistivity, low length decay factor, high functionalizability and significant affinity for the electrodes. Such affinity in certain cases leads to the formation of hybrid-molecular magnets (HMM),^{132,151,178,179} interfaces with high spin-polarization. Such HMM are generated as a consequence of the molecule-surface orbital hybridization, which provides magnetic features significantly different than the properties of both isolated subsystems due the superficially enhanced magnetism by the chemisorption of non-magnetic molecules. HMM present comparable magnetic properties to the above explained SMMs, but also exist some significant differences which need to be discussed. While the magnetic moment is reduced, the coupling strengths and anisotropy energies are increased, consequently increasing both coercive field and Curie temperature. Besides, HMM show higher blocking temperatures than SMM, thus being able to operate at temperatures above RT, fundamental capability to develop functional devices unlike the SMM. Examples of HMM can be coronenes or graphene islands on $\text{Ir}(111)$,¹⁷⁹ Zn methyl phenalenyl between Cu and Co layers¹⁵¹ or phthalocyanine molecules on Fe/W(110).¹⁷⁸

Different single-molecule spintronic devices have been developed employing both families of platforms. Spin-valves minimized at the molecular level are the most representative examples, since they operational simplicity have provided the first examples of molecular Spintronic architectures.^{180–183} Such single-molecule devices, analogous to the classical spintronic device, contain at least two magnetic subsystems (electrodes or molecule) and tune their electrical resistance for different mutual alignments of the magnetization interplay between the electrodes or between the molecule and one or the two electrodes. Such devices can be developed employing both device families. As example of using non-magnetic molecules, can be found C₆₀ fullerene¹⁸⁴ or octanethiol¹⁸⁵ based junctions sandwiched between Ni electrodes, CNT¹⁸⁶ junction between metal-LSMO contacts as well CNT trapped between Permalloy contacts.¹⁸⁷ Such devices show very large MR effects, transforming spin information into large electrical signals. Spin-valves also can be performed using magnetic molecules. In such cases, a magnetized electrode inject spin-polarized electrons to the magnetic molecule and depending the molecule's and magnetized electrode polarization alignments, the current will be tuned following the mechanism summarized on Figure 1.23. Examples of such devices can be found on SMM based on Tb(III) molecules sandwiched between CNT.^{188,189} SMMs based in double metallocene¹⁹⁰ or metalloporphyrins¹⁹¹ junctions are predicted as devices with outstanding spin-filtering capabilities since only parallel spins to the molecular magnetization can flow through the SMM allowing to the current displays, for a time equivalent to the relaxation time.

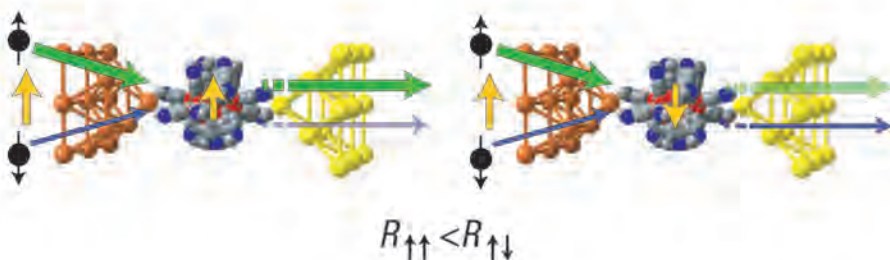


Figure 1.23: Spin valves based on molecular magnets. Yellow arrows represent the magnetization direction. Parallel configuration (left) of the magnetic polarized source electrode (orange) and molecular magnetization, with diamagnetic drain electrode (yellow). Spin-up majority carriers (thick green arrow) are not affected by the molecular magnetization, whereas the spin-down minority carriers (thin blue arrow) are partially reflected back. Antiparallel configuration (right): majority spin-up electrons are only partially transmitted by the differently polarized molecule, whereas the minority spin-down electrons pass unaffected. Assuming that the spin-up contribution to the current is larger in the magnetic contact, this configuration has higher resistance than that of the previous case. Adapted from Bogani et al.¹⁶³

Single-molecule spin transistors^{192–197} or spin resonators¹⁹³ also have been developed. In different works, they were designed using magnetic molecules, like SMM, trapped between two non-polarized tip and substrate STM electrodes. Thanks to this approach were proved different phenomena affected by the spin of the junc-

tion,^{192, 194–198} such as Kondo effect,^{194, 195, 198} magnetic anisotropy,¹⁹⁶ the first quantum tunneling current detection through a SMM¹⁹⁷ or the well-known Coulomb blockade.^{194, 197} Single-molecule spin transistors also were tested using SMM based on Tb(III) complexes on CNT^{188, 189, 193} (see Figure 1.24 left panel) or directly trapped in three-terminal break-junction devices¹⁹² (see Figure 1.24 right panel) which integrated gate control.¹⁹⁹

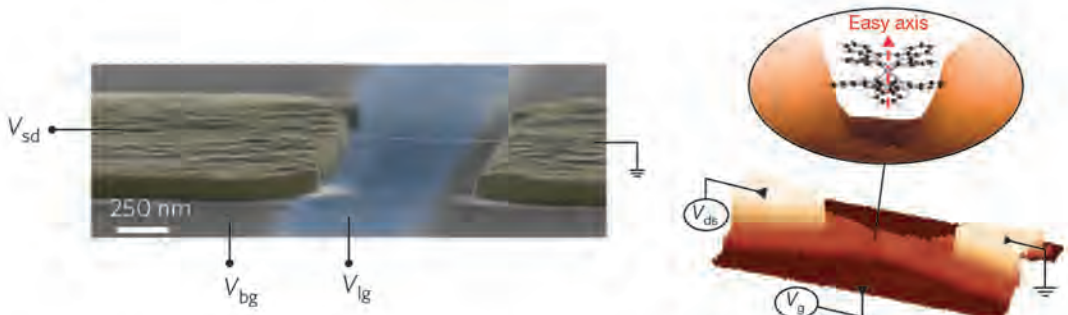


Figure 1.24: (False-colour SEM image of a CNT NEMS with local metallic (V_{lg} , blue) and Si^{++} (V_{lg} , grey) backgate (left). Adapted from Ganzhorn et al.¹⁹³ 3D extrapolation of a SEM image showing the most favorable structure of the SMM based transistor (right). Inset: schematic zoom of the nano-gap shows the molecular structure of the TbPc_2 SMM and its easy axis. The charge state of the ligand read-out dot can be controlled by the gate voltage, V_g , and the voltage difference between the electrodes is controlled through the drain-source voltage, V_{ds} . Adapted from Vincent et al.¹⁹²

1.3.1.4 Spintronic surface effects: SOC and Rashba splitting

The Spin-Orbit Coupling (SOC) is a relativistic magnetic effect occurred in the absence of an EMF, consequence of the interaction between the intrinsic magnetic moment of the electron and the magnetic field seen in its orbital motion around the nucleus. The SOC increases with the nuclear charge so that, for heavy atoms is more representative. The consequence of such effect is the mixing of zero-order states of different multiplicity.

SOC interaction induces many interesting phenomena in surfaces, such as the spin-Hall effect,²⁰⁰ topological insulators and magnetoelectric effects,^{124, 134} but the most significant phenomenon happens under the application of an external electrostatic potential, effect discovered by Rashba²⁰¹ and called Rashba-splitting.^{201–205} Mainly, the electrons moving near the surface or interface see the potential gradient as a magnetic field, which couples with the spin. In the presence of an electrical current J (green arrow in Figure 1.25) along the x-direction, the *Fermi Surface* (blue circle in Figure 1.25) is displaced along the same direction. Electric field couples to the spin of itinerant electrons since they moving in momentum space, as a consequence the electrons experience an additional spin-orbit field (thin red arrows in Figure 1.25) causing a non-equilibrium redistribution hence a broken inversion symmetry. The spins are now momentum dependent due to SOC (nonzero spin density)

showing *in-plane* spin-polarization perpendicular to the applied electrical current (*red arrow* in Figure 1.25).

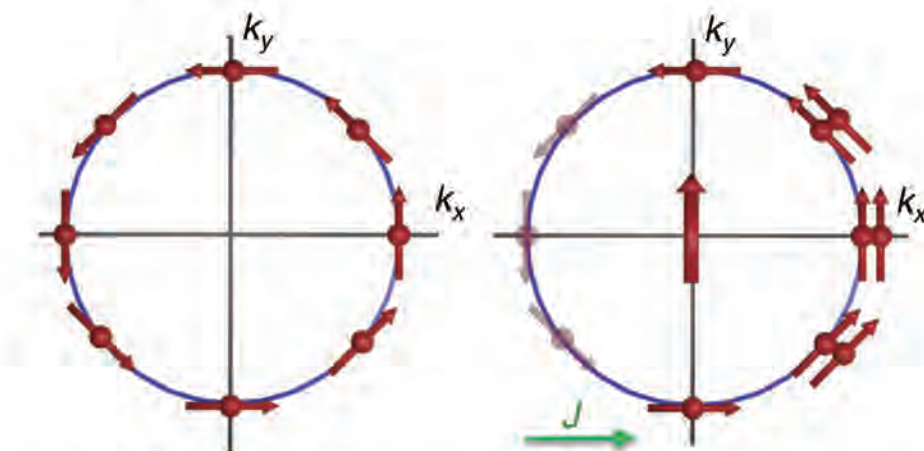


Figure 1.25: Rashba spin texture for one of the chiral states in equilibrium with zero net spin density (left). Non-equilibrium redistribution due an applied EEF resulting in a nonzero spin density due to broken inversion symmetry of the spin texture (right). Adapted from Sinova et al.²⁰³

As a consequence of such band-splitting, is generated the mixing of the minority and majority spin states and lifts the angular momentum degeneracy of the electronic levels, molecular orbitals or bands in atoms, molecules or solids, respectively.

Experimental studies on the Rashba effects reported for surfaces of metals such as Au(111), Ag(111), or Bi(111).²⁰⁰ And also for alloys such as Ag/Au(111) Bi/Ag(111) and Sb/Ag(111) and semiconductor heterostructures.^{206, 207} On Au and Bi surfaces the SOC interaction of the free electron, is generated an anisotropic magnetization due unbalanced topological surface states, known as spin-texture, phenomenon detectable using photoemission spectroscopic techniques like ARPES.^{208–213}

Moreover, in magnetic systems the magnetization has preferential directions since the interplay, through the SOC, with the underlying ionic lattices. This magnetic anisotropy energy (MAE)²¹⁴ is, both from a fundamental point of view and technological,^{215–217} one of the most important properties of magnetic materials. Large MAEs are desired for the development of high density magnetic data storage, and nowadays exist noteworthy research to find the design of optimum nanoscopic magnetic structures.^{218–221}

Is important to highlight that for the development of spintronic devices,²⁰⁵ SOC and Rashba effects can be essential since the magnetic anisotropy can be used as spin-polarized current source under an applied electrical current for both magnetic surfaces or non-magnetic with free electrons like Au.

Chiral structures like DNA show SOC effects, despite being organic structures without any metal inside. Many theories and models have been developed to explain such effect.^{222–225} The most extended one is the following²²⁵ considering an electron

moving along a one-dimensional helical path embedded in three-dimensional space. Under such premise and treating the spin's degrees of freedom quantum mechanically and the translational motion treated classically, only a little rotation²²² of the spin can be expected when an electron traverses a helix consisting of several turns (thus, suppressed SOC effect); but since electrons can hop between adjacent sites along the helix with hopping amplitude J or vertically to the N^{th} neighbor with hopping amplitude (see Figure 1.26), the SOC interaction is assumed²²⁵ due the associated electron motion, which is representative only for NN sites affecting only the NN bonds and not the axial bonds.

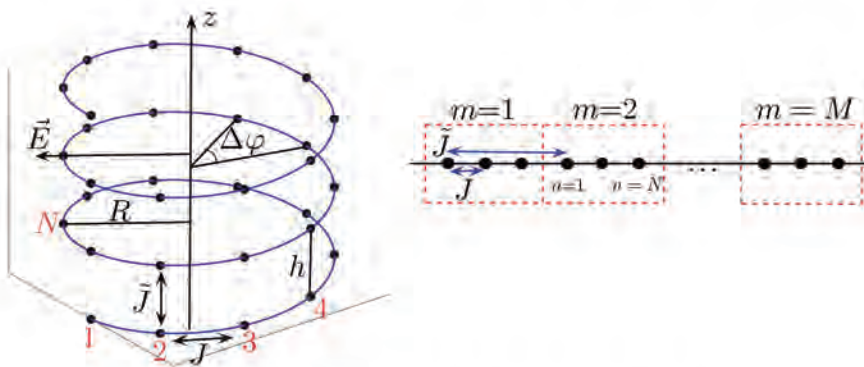


Figure 1.26: Tight-binding model of a single helical molecule with radius R , pitch h , and twist angle $\Delta\varphi$ (left). Hopping amplitude is J . Mapping of the model based on one-dimensional chain of M unit cells, each containing N sites (right). Adapted from Matityahu et al.²²⁵

1.3.2 Electric fields and molecules

EEF is one of the force fields which presents several uses due its interaction with molecules, examples of that can be find in the most classical and usual applications as the Stark Effect^{226–228} or the promotion of Electron Transfers, both widely used in the field of molecular spectroscopy;^{226, 228} obtain elicit spin-polarized conductivity;^{224, 229} electric pulses through a STM tips to promote molecular isomerization processes^{113, 230–233} and induce spin-crossover transitions in some molecular complexes²³⁴ or redox reactions.^{235–239} However, EEF never have been involved extensively in the field of reactivity, where developing new and more-efficient ways to control reactions is a constant quest for chemists. Understanding the chemical reactions as processes where are involved electron transfers between atoms or molecules and/or rearrangements of the positions of nuclei, the EEF represent a direct and very intuitive way to affect such processes in a kinetic and thermodynamic way if these processes are simplified as scenarios of “charged particles under constant motion”. Such interplay between EEF and charged particles has been predicted theoretically^{240–246} and also experimentally very recently. These works sustain that the transition state (TS)^{247, 248} can be electrostatically stabilized due the substantial decrease caused by the EEF, therefore is facilitating (accelerating) the reaction^{249–252} and affecting significantly to the rate constant (k) as has been pointed by different theoretical works.^{240–242} This is a very appealing concept, since the thermodynamics of the TS theory predicts an Arrhenius dependence (see *Expression 1.21*) of k on the energy barrier imposed by the TS (G^\ddagger) which implies that a decrease of just several tens of meV in ΔG^\ddagger can accelerate the reaction by an order of magnitude,

$$k \propto \exp\left(\frac{\Delta G^\ddagger}{RT}\right). \quad (1.21)$$

Shaik and co-workers studied widely the interplay between EEF and the TS adducts during the chemical reaction process, in their model is assumed that some covalently bonded chemical species can be understood as combinations of resonance reaction contributors of the transition state,^{240–244, 251, 253–255} name received by molecular structures which the electrons of chemical bonds can be localized in various ways to distribute the charge. Using such model the bond of an ideal AB molecule with a covalent bond, is the consequence of the dynamic equilibrium of several possible charge-separated resonance contributors,^{251, 253, 254} as *Expression 1.22* tries to summarize.



Assuming in the proposed model by Shaik, during a reaction the EEF appropriately orientated can affect the complex equilibrium of the charge-separated resonance contributors by electrostatically stabilizing them, and therefore increasing their degree of resonance,^{240–243, 254} thus affecting to the bond energy (Figure 1.27).^{251, 253} As a consequence it affects to the global stabilization of the molecule or its transition state, resulting in a accelerated chemical reaction.^{240, 243} The described mechanisms tune the chemical reactions in a strictly different way for the redox (or electroac-

tive) and the non-redox processes. In the former, the EEF tune the energy levels of electrons in reactant molecules allowing the electron transfer between the electrode and the molecules. On the contrary, when the involved chemical species do not present electroactive properties, the EEF affects the reaction by changing local concentrations of the reactants molecules, or by bringing charged groups molecules cooperatively close to each other as usually happens in biological processes.

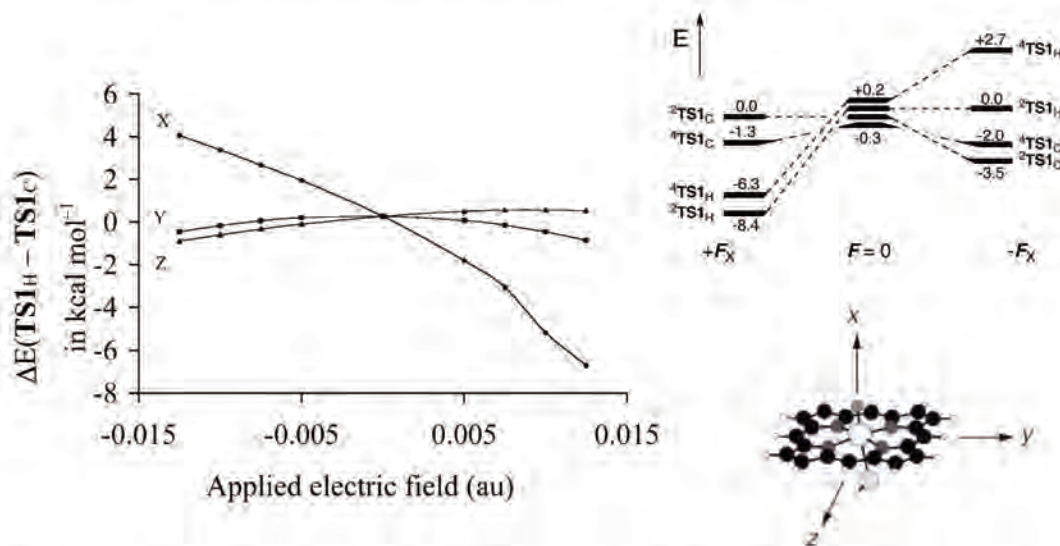


Figure 1.27: (Left) Relative energies of the bond activation TS ($TS1_H$ and $TS1_C$; these are average energies of the spin states) under the influence of applied electric fields of different strengths, x , y , z -orientations and directionality; x is the S-Fe-O axis, perpendicular to the porphyrin plane. (Right-top) The relative energies of the four transition states, ${}^2, {}^4 TS1_H$ and ${}^2, {}^4 TS1_C$, in a zero field ($F=0$, center), and in x -directed fields of $F_x = +0.01$ au and $F_x = -0.01$ au. (Right-bottom) Cartesian axes. Adapted from Shaik et al.²⁴³

Thanks to all the developed theory background can be assumed that the application of an EEF stabilizes electrostatically the TS and catalyze the reaction, the concurrence of these three concepts gave birth to “electrostatic catalysis”^{245,246,256–258} defined usually as the study to manipulate chemical reactions applying electric fields, being the the least developed form of catalysis in synthetic chemistry. Trying to establish this field at the non-biological chemistry level, several problems arise despite working in a polar environment such as water, since the local electrostatic fields can be substantially high (as much as tens of MV/cm) but their intrinsic isotropy can effectively quench the field’s directionality, thus muffling its effect over the relevant reaction coordinates. But under biological scenarios and presenting similar working conditions such as aqueous and polar medium in environments under a highly concentrations of electrolytes, enzymes can decrease the TS energy in a extraordinary efficient way overcoming this problem by creating cavities (or cages) with low-polarity active sites where charged residues are strategically located to create a directed *Local Electric Fields* (LEF) which orient the substrate, stabilizing the TS thus, catalyzing the reaction.²⁴³ For this reason electrostatic catalysis has

been hypothesized for several decades as a plausible mechanism for the enzymatic catalysis taking place in the active sites of many biological structures such as proteins,^{243, 256, 257, 259} which becomes a highly efficient nano-reactor capable of catalyzing non-activated chemical reactions under ambient conditions through controlling locally the electrostatic fields due the LEF;^{260–263} although the *in-situ* mechanisms remain unstudied, several theoretic studies^{257, 260, 263, 264} point that the EEF catalytic effects on the enzymatic reactions through the TS stabilization (exemplified in Figure 1.28) as a consequence of the interplay between the enzyme's cavity LEF and the applied EEF.^{246, 257, 258, 263} In fact, the enzymatic complexity can not merely be reduced to electrostatic fields,^{240, 241, 246, 265–269} example of that are the recent works in energetics which have suggested that spin-state selectivity might also play a role along the electrostatic field in enzymatic catalysis.^{265, 268} The importance of spin alignment in well-known artificial heterogeneous catalytic process has been indeed evidenced,^{266, 267, 269} suggesting that spin-dependent ET processes in redox enzymes might lead to additional TS stabilization through stabilizing the spin-polarized intermediates that typically evolve in the catalytic cycle of redox enzymes.²⁴⁶

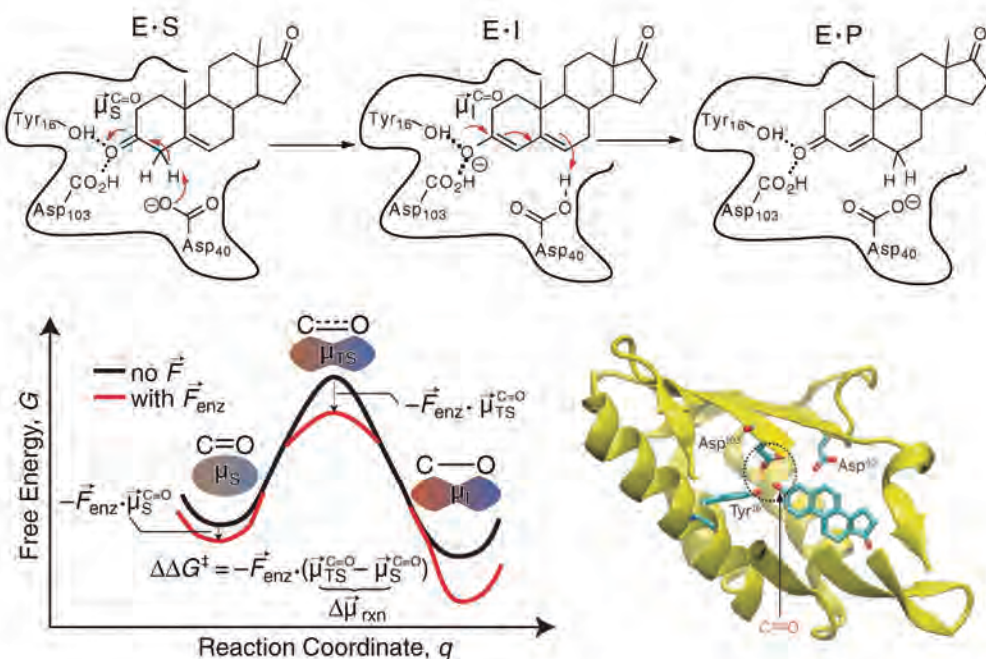


Figure 1.28: (Top) The chemical mechanism of ketosteroid isomerase. In the first step, Asp⁴⁰ removes an a proton from the steroid to form an enolate, stabilized by two H-bonds from Tyr¹⁶ and Asp¹⁰³. This transformation results in an increase of the dipole moment along the C=O bond. E, enzyme; S, substrate; I, intermediate; P, product. (Bottom-left) The effect of an EEF from the organized environment of an enzyme active site F_{enz} on a reaction's activation barrier (ΔG^{\ddagger}) $\vec{\mu}_S^{C=O} - \vec{\mu}_{TS}^{C=O}$ dipole of substrate's C=O bond; $\vec{\mu}_{TS}^{C=O}$ dipole of transition state's C=O bond. (Bottom-right) The structure of the active site of a ketosteroid isomerase with the binned enolate. Adapted from Fried et al.²⁵⁷ and Wu et al.²⁶³

Understanding how the electrostatic catalysis affects k through the LEF thanks the cage-like structural “nano-reactors” cavities is not tribal because enzymes are able to catalyze the most demanding reactions in biology with tremendous interest in bio-manufacturing.²⁷⁰ Industrial bio-manufacturing is one of the pillars of today’s world economy making its way to continue with a sustainable development. Its future goes inevitable through further advances in the design of biocatalysts with enhanced capabilities for technological applications. The reaction rate enhancement enzymes can achieve is as much as 10 orders of magnitude higher than the same reaction occurring in solution. Putting aside the technological perspective, from a biological point of view any study which can contribute a better understanding of enzymatic mechanisms would allow, for instance, interfering in the countless enzymopathies associated with anomalous variations in the enzymatic activity.²⁷¹

The above facts are too strong to be ignored and, therefore, there are two milestones needed to reach to advance in the *electrostatic catalysis field*: the development of a ***robust platform***, to allow the study and the practical application of the EEF effects over reactions; as well as, use it to understand of the ***mechanistics*** behind the affected reactions by the EEF. Achieving both, not only the EEF may be used to accelerate chemical reactions employing a force (electrical) field as a catalyst, but also the mechanics of the enzymatic processes will be elucidated and would be improved using the EEF.